

2024

Shape Morphing Bolstering

Graduation Project

Student: Max Nijhuis
Client: Jaguar Land Rover
Mentor: Dr. Sepideh Ghodrat
Mentor Client: Dave Withey
Chair: Prof. dr. Peter Vink

STUDENT

Max Nijhuis 4618149

CLIENT

Jaguar Land Rover

UNIVERSITY

Delft University of Technology
MSc Integrated Product Design
Faculty Industrial Design
Engineering

MENTOR

Dr. Sepideh Ghodrat

CHAIR

Prof. dr. Peter Vink

CLIENT MENTOR

Dave Withey

DATE

12-02-2024

Table of Contents

1. Introduction 6
- 1.1 Project Introduction 6
- 1.2 Knowledge Gap 7
- 1.3 Relevance to JLR 7

2. Bolsters 9
- 2.1 Introduction 9
- 2.2 Current system & Problem definition 11
- 2.2.1 Lay out 12
- 2.2.2 Load Bearing 13
- 2.2.3 Response time 13
- 2.2.4 Adjustability 14
- 2.2.5 Pressure Distributions 14
- 2.3 Comfort 20
- 2.3.1 What makes a bolster comfortable? 21
- 2.3.2 Pressure Distributions 22
- 2.4 Conclusions & Design implications 23
- Main Takeaways: 24

3. Materials 28
- 3.1 Introduction 29
- 3.2 Different kinds of SMM's 29
  - 3.2.1 Shape Memory Alloy (SMA) 30
  - 3.2.2 Shape Memory Polymers (SMP) 35
- 3.3 HASELS 38
- 3.4 HASEL- vs SMA Actuators 41
- Main Takeaways 45

4. Conceptualisation 50
- 4.1 Introduction 51
  - 4.1.1 Explanation design cycle 52
  - 4.1.2 Cycle within a cycle 53
  - 4.1.3 Material driven design 54
  - 4.1.4 Literature Conclusion & Design Goal 55
  - 4.1.5 Reflection on Literature Findings 56
- 4.2 Pressure Distribution Test 57
  - 4.2.1 Introduction 57
  - 4.2.2 Pilot Test 59
  - 4.2.3 Test observations & Questionnaire Results 59
  - 4.2.4 Data Analysis 59
  - 4.2.5 Conclusion & Limitations 62
  - 4.2.6 Design Recommendation 63

5. Ideation & Embodiment 66
- 5.1 Introduction 67
  - 5.1.1 Ideation 68
  - 5.1.2 CAD Model Analysis 70
  - 5.1.3 Model Iterations 73

6. Concept Overview 92

7. Evaluation 100
- 7.1 Validation 101
- 7.2 Conclusion 103
- 7.3 Recommendation 104

Appendendices 107

1. Introduction



RANGE ROVER AD FOR AIRSUSPENSION (JLR, 2993)

1. Introduction

1.1 Project Introduction

Since the introduction of large-scale automotive production in 1908, research into the shape and performance of seats has made steady progress alongside innovation in car interiors (Liamadis, 2013). Mostly lead by innovation in production techniques and material science, improvements in seating comfort have followed through at a steady pace through the years (Recaro, 2016). However, as is the case with most car components, seating innovation comes at a cost of added product complexity to the detriments of weight and power consumption (Daffner, 2021). While there are many methods to objectify seating performance, some of which will be addressed in this research, on the consumer side “good” is often determined by a seats (subjective) comfort and other functionalities, such as heating and massage function, as is described in a review by Farah (2019). Designers are tasked with finding a balance between these customers’ needs and external (space, weight) limitations to their design. The need for electrification has made it clear that innovation with bulkier and more complex design as a result is not a sustainable way forward, as this often results in a higher overall consumption of energy used. With no internal combustion engine (ICE) to power a vehicle, energy becomes a more valuable commodity and must therefore be regarded as such in each step of the design. Automotive manufacturers, much like other large industries, should adhere to limitations of battery technology. The need for increased efficiency in design seems clear, as both emodied energy and energy consumption must decrease



FIGURE 1: RANGE ROVER CLASSIC INTERIOR (JLR, 1972)

to reduce overall CO2 emissions, but this is not yet set through in all aspects of automotive production. As an example, first being introduced by Mercedes-Benz in the early 1990’s, pneumatically adjustable seat systems still largely rely on the same technology they did upon their introduction, namely a small pneumatic pump, an airbag and a series of valves (P. Reed et al., 1991). Progress in material science means that since the 1990’s a large spectrum of “new” materials possibly suitable for redesign of these systems in a potentially more efficient manner have been introduced, yet much of this seems largely unexplored, Possibly, there are concerns among manufacturers regarding the cost-effectiveness of investing in these novel materials.

This research focusses on the integration of shape memory materials (SMM), which are characterized by their ability to change shape, stiffness, or other properties in response to external stimuli such as temperature, pressure, or electrical current. Using these morphing materials, like shape memory alloys (SMA), in bolsters represents an uncharted territory, that could potentially lead to a revisiting of adjustability systems in seating design. By exploring these innovative materials and their adaptability, this thesis aims to bridge the gap between traditional seat mechanisms and contemporary, efficient designs.

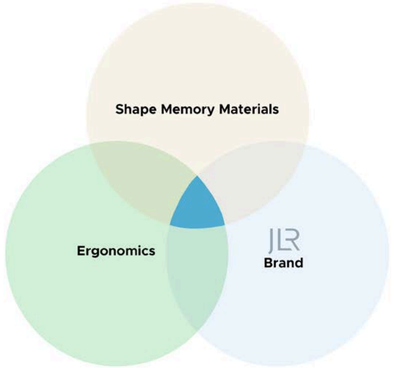

FIGURE 2: THE RESEARCH GAP OF THIS PROJECT

1.2 Knowledge Gap

While significant research exists on morphing materials and car seat ergonomics separately, a notable knowledge gap can be seen in the lack of sources that integrate these two topics. Despite there being many studies on morphing materials’ adaptability and the intricacies of car seat ergonomics, there’s a lack of literature that merges these areas to develop novel solutions.
The absence of support from the industry could potentially be a contributing factor to this situation regarding the implementation of SMM. The research goal is to bridge this gap by aiming to enhance seat comfort and performance through the creation of a shape memory material-based bolster system (Figure 2). This can be characterized as a system that achieves particular mechanical responses through temperature variations, in contrast to a conventional system that relies on air pressure. By researching the potential of morphing materials in the context of ergonomic seat design, this research aims to find a novel approach towards car seat adjustability.

1.3 Relevance to JLR

Within the automotive industry, many Original Equipment Manufacturers (OEMs) have adopted similar parts, features, and materials for their seats. This

has posed challenges in distinctiveness for brands like JLR aligning with its commitment to creating unique vehicles, as mentioned in their mission statement (JLR, 2023). It is assumed that this similarity in seating design results from years of OEMs using similar sources, use cases and competitor research as source for their product development. This perhaps has lead to the development of products that are progressively more alike to those offered by their competitors and thereby posing a challenge to differentiate and provide a unique offering distinct from competitors

The dynamic automotive landscape is subject to technological advancements and evolving regulations, which means the role of the occupant of vehicles is changing. Since the act of driving is taken over by automation and exterior design is increasingly influenced by external factors such as regulations, societal concerns (safety) and infrastructure, it could be argued that the interior space of a vehicle is becoming a more important factor in standing out from the competition. Investigating new materials, despite initial costs, is a potential opening for JLR to set itself apart from competitors, while aligning with their



FIGURE 3: NEW AND OLD DEFENDER (JLR, 2020)

mission “to deliver exceptional customer experiences”.

This thesis examines how integrating novel materials, aligns with JLR’s wishes and demands for seating design, while offering a potentials method for the brand to differentiate from its competitors, while remaining true to its values and heritage.

2. Bolsters

2.1 Introduction

In pursuit of increasing comfort and seating performance in automotive design, the bolster section of this report consists of an investigation into the existing bolster system of the Range Rover L460 front passenger seat (Figure 4). Its aim is to not only create a detailed understanding of the workings and individual components of the current system, but also use this knowledge towards the creation of a more adaptive and efficient system based upon most recent leading material science and human ergonomics science.

This study involves a general examination of the performance of the current system, a comfort section in which subjective comfort in relation to seat bolsters is discussed and a conclusion in which recommendations are given for further design.

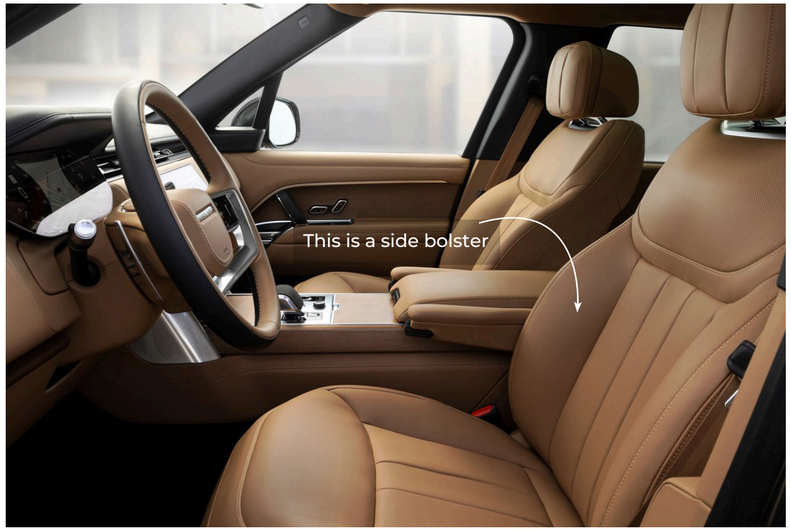

FIGURE 4: L460 FRONT SEAT (JLR, 2020)

2. BOLSTERS

2.2 Current system & Problem definition

The Range Rover L460 seat (Figure 5) has an extensively adjustable design. The seat consists of pneumatic and servo-motor driven components that allow for x-way adjustment over 2 axes. However, the system used to achieve this adjustability has multiple inherent challenges. Firstly, as highlighted by Dave Withey, seating innovation specialist at Jaguar Land Rover, the L460 seat's sophistication comes at the cost of high complexity and a high number of components, increasing the potential points of failure. This complexity not only rises the cost of production, but also makes the seat challenging in terms of repair and maintenance.

Additionally, while being very advanced in terms of ergonomic shaping for comfort, the pneumatic system mostly relies on passive components for pressure distribution (not considering the massaging system). This brings limitations in its ability to dynamically adapt to individual body shapes and preferences.



FIGURE 5: L460 SEAT VIEWS

Finally, the pneumatic system responsible for seat adjustments relies on heavy hardware that contributes greatly to the weight of the seat, therefore affecting its overall efficiency.

A redesign should address these limitations but also prioritizes safety, adaptability, simplicity, and user comfort.

2.2.1 Lay out

The seat features an adjustability system to change its contours which utilizing shape-memory alloy actuated valves, managed by a LIN-based control system, to activate 18 separate air cells (Figure 6). These air cells are strategically positioned across the lumbar, upper back, shoulder, and side bolster sections of the seat.

Moreover, the seat has a central power control module responsible for powering the electronic adjustability and pneumatic systems.

The material layering is as follows:

1. Leather Trim Cover
2. Heater Mat
3. Low Density PUR “Topper” Foam
4. PUR Foam
5 Air distribution layer

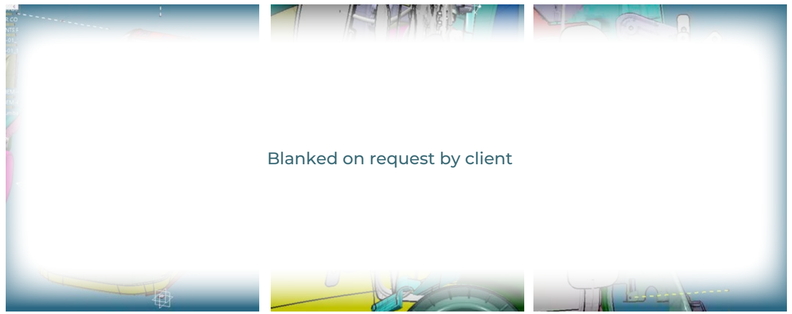

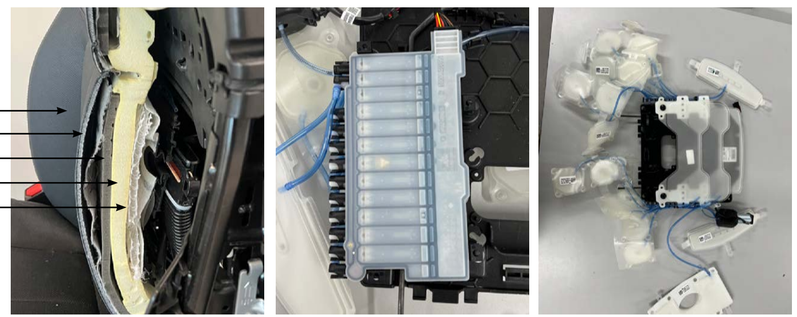

FIGURE 6: COMPONENTS OF THE L460 SEAT

2.2.2 Load Bearing

JLR tests durability of its cells by applying 250N of load evenly spread across 4 air cells with a total of 1330 hours run time. 1 cycle is described as travel from the fully unadjusted to 90% of maximum pressure then back to the fully unadjusted position (Figure 7). This is done in cycles of 20 minutes of continuous activation, with rest times of maximum 10 minutes in between. This does not necessarily provide peak force application data, but does suggest that each cell should be able inflate up to 90% pressure at a load of 62.5N (JLR, 2021).

In addition, the number of cycles done at unloaded at different temperatures is defined as follows for a sequence of 1000 cycles: 50% at +23°C, 25% at -30°C, 25% at +50°C. For each temperature state a minimum of 2.5 hours of soaking time is required and the frequency is limited to 60 cycles per hour.

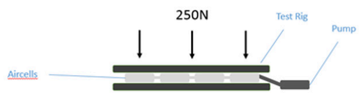

Figure 1 - Function Test Set-up

FIGURE 7: AIRCELL DURABILITY SETUP (JLR, 2021)

Force

In order to gain insight in the force application a a single cell, a short test was conducted by the author (figure 8). The maximum force applied by the cell of the side bolster is 2.8N at the most outer point of the cell. If we consider the cell a square shape, this gives us an indication of the mean force it can deliver:

Pressure = 2.8 N / 72 cm^2 ≈ 0.0389 N/cm^2
Total force = Pressure * Total surface area
Total force ≈ 0.0389 N/cm^2 * 288 cm^2 ≈ 11.21 N



FIGURE 8: TESTING FORCE APPLICATION

2.2.3 Response time

In testing (figure 9), at 12.6V and 0.02A (As specified by JLR Test procedure, see appendix A), response time is 8.8s for a single bolster airbag in an unloaded setting.

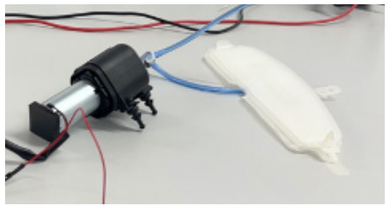

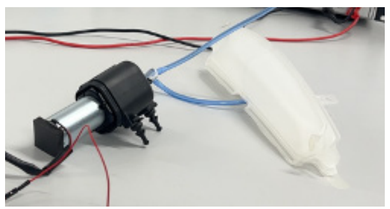

FIGURE 9: TESTING REACTION TIME

2.2.4 Adjustability

The seat bolster on the L460 offers 60mm adjustability across the dotted line shown in red on figure 10.

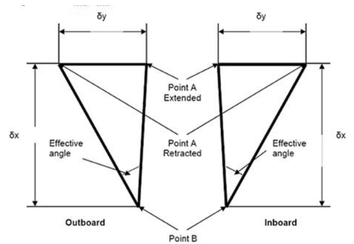

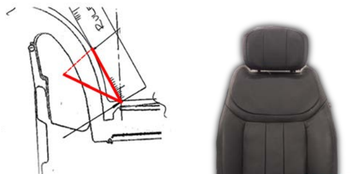

FIGURE 10: TRANSLATION RANGES

2.2.5 Pressure Distributions

This section of the research focuses on exploring pressure distribution in the bolsters of a JLR L460 seat.
Using a pressure mat, a test was conducted to investigate pressure points during short and extended sitting periods. While limited in scope with a single participant, this initial examination aims to confirm suspected pressure hotspots around the bolster area. Its findings act as a validation method for further more comprehensive research upon which the new bolster adjustability system will be designed.

Instrumentation

The LX210 was connected to the XSENSOR Pro V8 software to record pressure distribution on the backrest, particularly focusing on the side bolster area. Different sections of the backrest are divided into sections KT1, KT3, KT4a, KT6a, KT7 and KT8, with KT3 being the side bolster (Figure 11). The recording of pressure distribution is done at a resolution of 12.5mm and is measured in N/cm2 (Xsensor Corporation, 2021).

Method

Participants: The study involved a single participant who sat in a JLR L460 seat equipped with an XSENSOR LX210 pressure mat. The seat was conditioned overnight at an ambient room temperature of 21°C to optimize foam properties (D. Withey, Personal communication, 2023).

Seat

The L460 seat was placed on aluminum extrusion profiles with a seat pan height of 40cm. The angle between backrest and seat pan was set at 110 degrees approximately, to have a neutral and comfortable seating position (Kolich, 2003). The test was conducted with the seat tilted counter-clockwise by 8 degrees around the Y-axis, as illustrated in the provided axis system (refer to Figure 13). This tilting configuration aimed to simulate lateral G-forces and create a more realistic pressure distribution on the side bolster, mimicking the conditions experienced during dynamic movements in a vehicle.

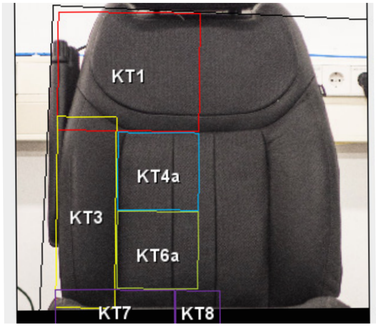

FIGURE 11: PRESSURE ZONES



FIGURE 13: AXIS SYSTEM

Procedure

The participant was asked to sit in the tilted seat for a duration of 15 minutes, allowing the foam in the seat to properly settle. During this time, the pressure distribution on the backrest was continuously recorded using the XSENSOR V8 software (Figure 14).



FIGURE 12: PRESSURE MAT ON SEAT

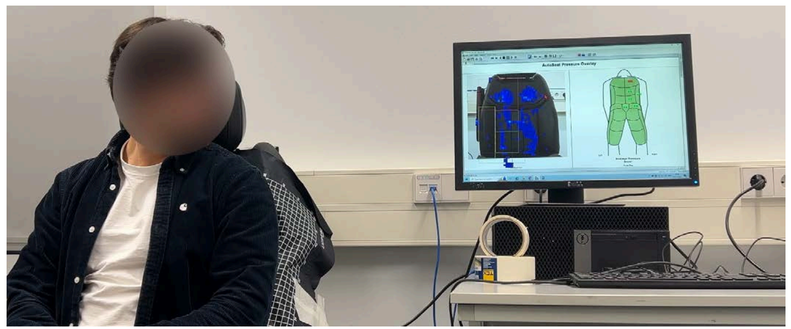

FIGURE 14: PARTICIPANT DURING TESTING



FIGURE 15: L460 VISUALISED AS A CAD MODEL

Data Analysis

The collected data were analyzed by the author to determine both the peak pressure distribution and the average pressure distribution over time. By analyzing both average and peak pressure distribution, an evaluation of the seat's performance in terms of comfort over time can be evaluated as well as short term discomfort through peak pressure points can be identified. This dual approach aids in refining seat design for better ergonomic support and user experience. Additionally, the pressure distribution imagery was imported into Blender, a 3D CAD software, to create an overlay with a 3D model of the seat's side bolster. This process enabled the visualisation of pressure distribution on a 3D model, allowing for a more practical understanding of pressure points on the seat's surface under simulated lateral forces (Figure 15).

Testing

Test 1: Short Duration Sitting (2 minutes)

The initial test involved a short duration of sitting (2 minutes) and revealed an absence of a clear peak pressure distribution (Figure 16 & 17). This observation was expected, primarily due to the limited duration not allowing sufficient time for the foam in the seat to settle.

The absence of clear peak pressure distribution in the short duration sitting test aligns with the expected behavior of foam settling and molding gradually over time. This phenomenon leads to a more uniform pressure distribution initially, as the foam adjusts to the participant's body contours.

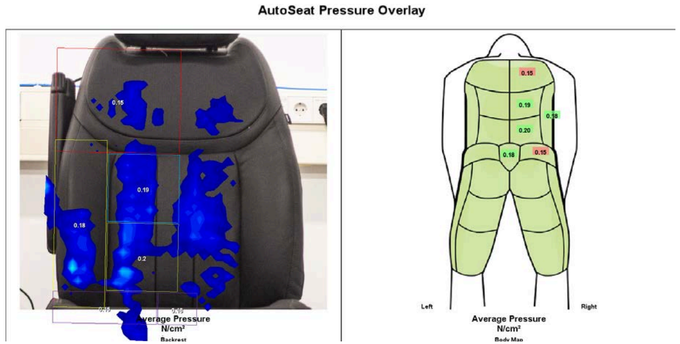

FIGURE 16: AVERAGE PRESSURE TEST 1

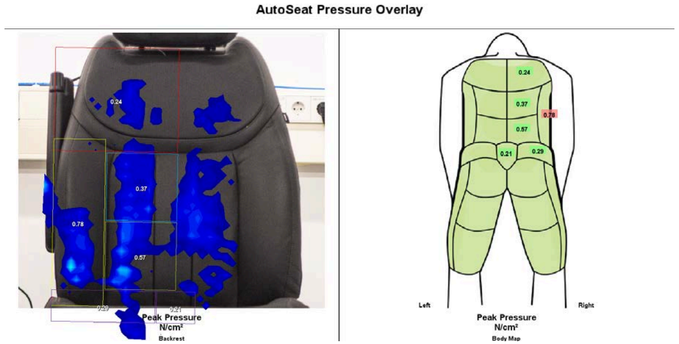

FIGURE 17: PEAK PRESSURE TEST 1

Test 2: Longer Duration Sitting (15 minutes)

In contrast to the shorter duration test, a longer sitting period demonstrated a notable shift in the pressure distribution pattern (Figure 18 & 19).
Peaks in pressure began to become more noticable, particularly in specific regions, such as the lower side bolster area.
Despite the appearance of these peaks, the overall pressure distribution remained relatively similar. This finding suggests that while prolonged sitting allowed for the development of noticeable pressure points, the general distribution pattern across the backrest remained consistent

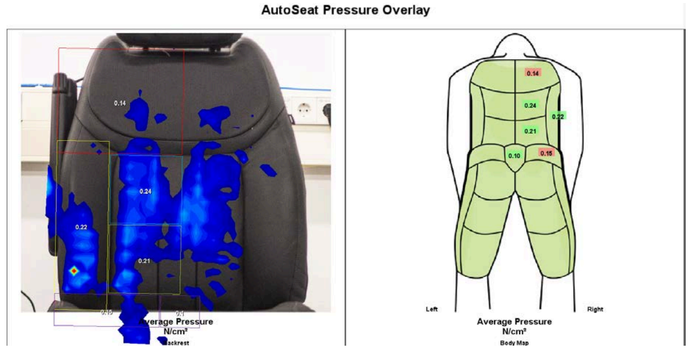

FIGURE 18: AVERAGE PRESSURE TEST 2 (NIJHUIS, 2023)

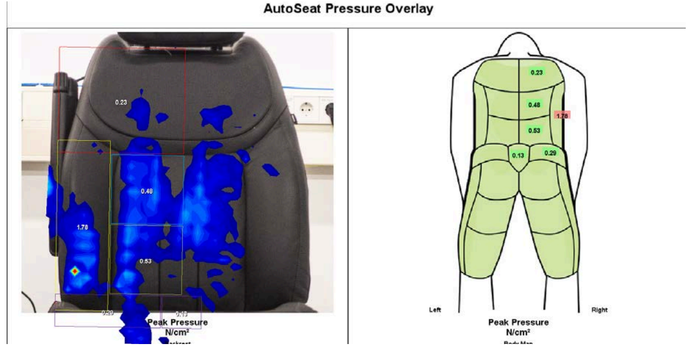

FIGURE 19: PEAK PRESSURE TEST 2 (NIJHUIS, 2023)

3D-Overlay

When modeled in CAD, we can isolate the bolster from the rest of the seat and examine how the recorded pressure distribution is distributed in 3D. This gives insight in to where a potential design would make most sense. We see that especially the lower section of the bolster is affected.

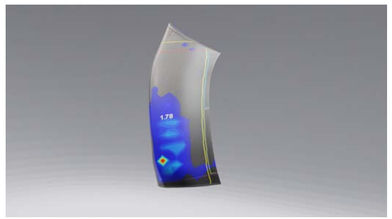

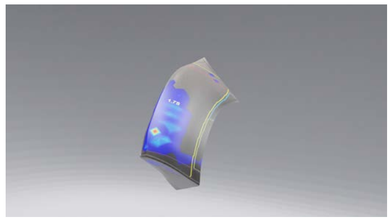

FIGURE 20: PRESSURE DISTRIBUTION ON BOLSTER IN 3D

Conclusion and Discussion

As the sitting duration increased, particularly in the longer test, distinct peaks in pressure became noticeable in specific area of the side bolster where the lower part of the rib cage touches the seat, as well as where the elbows are in contact with the bolster. These pressure peaks show localized areas of higher-pressure concentration.

This initial test with a single participant (n=1) provides valuable insights into potential hot spot areas on the bolsters. However, due to its limited sample size, it's not comprehensive enough to serve as a standalone basis for academic research. Instead, this serves as an important preliminary step, confirming prior suspicions and setting the stage for more comprehensive and detailed testing in the prototyping phase of the project.

In consideration of further research, it is hypothesized that by increasing the sample size of participants with diverse body sizes and shapes, the pressure distributions across the bolster's surface are assumed to show reduced centralized peak pressure and a more uniformly distributed average pressure. This expectation stems from the understanding that the contact patch on the surface is likely influenced by the body shape of the occupant, therefore potentially resulting in significant variation among participants.

2.3 Comfort

In car design, seats need to cater not only to the intended users but also match the overall style of the vehicle within the brand's context (Van Kamp, 2012). When it comes to seat design, there's a noticeable trend: the sportier the car, the more pronounced and contoured the seats tend to be. These seats often have prominent side bolsters, both upper and lower, giving a "bucket" seat effect that provides excellent lateral support for occupants.

Aggressive side bolsters excel in keeping occupants secure during fast turns, enhancing safety, support, and stability compared to less contoured seats. Bolsters also play a role in how roads and the act of driving are experienced by the occupant (Vink, personal communication, 2023). However, they do present challenges that might limit their suitability for other types of cars.

One significant challenge is the difficulty in getting in and out of the seat. The firm and raised structure necessary for stability during dynamic driving can pose obstacles, especially for individuals with limited mobility. Using seats with aggressive bolsters often requires adjustments in posture and more effort to avoid discomfort.

When considering inclusivity, these seats involve a trade-off in design to accommodate various body sizes. The rigid structure makes it challenging to create a seat that fits well for most people while ensuring safety, comfort, and proper ergonomics. Larger individuals might feel cramped due to the seat's inflexibility, while smaller individuals might not feel adequately supported, increasing the risk of sliding around.

On 31/10/2023, during the authors visit to Jaguar Land Rover in Gaydon, UK, robotic arms could be seen that are used with an SAE J826 H Point manikin to mimic the cycles of ingress/egress and pressure distribution on all variants of their seats (Figure 21). This is done to represent the weight and contour of a 10th, 50th & 95th percentile adult male (ETD - Technical Trading, 2021).

Seats tailored for luxury, such as the L460 seat, prioritize adjustability over pronounced bolsters. As a result, they facilitate easier entry and exit, accommodating a broader range of users. However, they compromise on the snug fit and lateral support typical of bucket-style designs (Figure 22).



FIGURE 21: ROBOTIC ARM WITH MANIKIN AT JLR



FIGURE 22: BUCKET TO LUXURY SPECTRUM OF SEATS

2.3.1 What makes a bolster comfortable?

Variation in seat design philosophy largely depends on what designers estimate as user preference. Nonetheless, emerging technologies offer promising possibilities to minimize these compromises in seat design. The research primarily centers on the L460 seat, positioned within the luxury spectrum, and therefore prioritizes comfort, but also explores optimizing lateral support for maximum snugness and fit while driving.

It is difficult to objectify what determines comfort, however there are several generally accepted factors that contribute to comfort, as described by Looze et al. (2003): "Comfort is a construct of a subjectively defined personal nature, it is affected by physical, physiological and psychological factors and it is a reaction of a person interacting in the environment".

Le et al. (2014) categorizes this into three main elements: the seat itself, the occupant, and the interplay between the two.

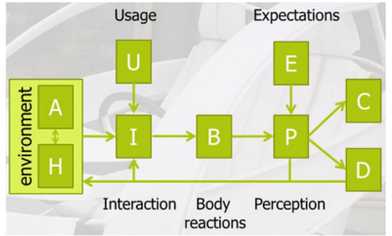

FIGURE 23: COMFORT MODEL BY VINK AND HALLBECK (2012)

This interaction is explained in the comfort model created by Vink and Hallbeck (2012), depicted in figure 23. In the model of Vink & Hallbeck (2012), the artifact (A) and human (H) within the environment interact (i), generating an effect on the body (B). The expectation (E) and the body's response create a perception (P) leading to the decision of comfort (C) or discomfort (D).

Regarding this interaction (i), while numerous factors contribute to overall perceived comfort within a seat, this research narrows its focus to bolsters. Consequently, efforts are directed toward minimizing external variables within this specific area during testing by maintaining limited seat and body parameters (SAE J826 H Point manikin).

Moreover, Kong et al.'s study in 2012 emphasizes the distinction between the absence of discomfort and the actual sensation of comfort. They are considered as separate entities that require individual attention.

As described in research by Zhang, Helander, Drury, (1996) the term 'comfort' typically is linked to a sense of relaxation, well-being, and aesthetics. On the other hand, 'discomfort' relates more to the aspects of 'suffering', often tied to biomechanical factors, such as joint angles and range of motion, resulting in sensations of pain, numbness, and stiffness. These discomforting feelings tend to escalate with prolonged tasks and fatigue.

2.3.2 Pressure Distributions

Addressing the bodily reaction to side support comfort, Van der Voort's study *"Comfortable Side Supports in Automotive Seating"* in 2018 highlights the significant influence of shear stresses exerted by the body on the bolsters during lateral acceleration.

According to Van der Voort, these shear forces exert themselves at perpendicular angles to the surface where the seat and the occupant's skin make contact. They're influenced by factors like occupant size, weight, bolster shape, and vehicle dynamics. It's essential to note that these forces can't be entirely eliminated; otherwise, the occupant wouldn't receive lateral support. However, it's crucial to consider how these forces distribute across the contact patch's surface.

When aiming for comfort, the average, maximum, and gradient pressure (the rate of pressure change) become most important. Van der Voort's work in 2018 details the impact of these variables, as outlined in Table 1. Higher values of

Tolerance sitting time [min]	< Maximum pressure [N/cm²]	< Average pressure [N/cm²]	< Pressure gradient [A(N/cm²)/ B(N/cm²)]
100	5	0.6	2.5
150	3	0.5	1.5
240	1.5	0.4	0.5

TABLE 1: TOLERANCE MEASUREMENT (VAN DER VOORT, 2018)

these forces typically correlate with lower comfort levels.
Research by Zenk et al. (2007) shows that there's a significant correlation between total discomfort and both maximum and averaged discomfort concerning side bolsters (Table 2). The findings indicate a notably higher coherence between total discomfort and maximum discomfort in comparison to averaged discomfort. According to Zenk et al, this shows how maximum discomfort affects total overall perceived discomfort and should therefore be kept to a low.

	BACKREST		SIDE BOLSTERS	
	Maximum Discomfort	Averaged Discomfort	**Maximum Discomfort**	Averaged Discomfort
r correlation coefficient	**0,88**	0,87	**0,88**	0,86
R^2 determination coefficient	**0,77**	0,75	**0,78**	0,73

TABLE 2: CORRELATION IN DISCOMFORT (ZENK ET AL., 2007)

This phenomenon can be understood through the human tendency to overlook subtle variations in a consistent state but easily perceive significant changes (Halprin, n.d.).
The test combined a Body Map with a CP50 scale combined for participants to rate their discomfort (Figure 24).

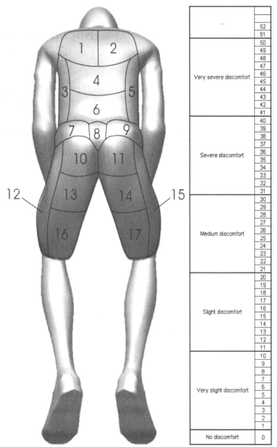

FIGURE 24: CP50 BODYMAP (ZENK ET AL., 2007)

2.4 Conclusions & Design implications

Conclusion

In the research conducted by the author, a detailed exploration of the Range Rover L460 front passenger seat's bolster system has shown several areas for improvement of seating comfort and performance.

While the current system demonstrates sophisticated pneumatic and servo-motor driven mechanisms, its complexity poses challenges in design, repair, and maintenance.

An important aspect of human centered design (HCD) is to create a design tailored to the specific needs, preferences, and capabilities of the users (Harte et al., 2017). In this research, this definition of user-centric solution and inclusive design is limited to the ergonomic adjustability side to remain within the scope and time frame of the project. In the research conducted by the author, new insights regarding the limited adaptability of the seat were made. Especially its inability to conform dynamically to individual body shapes and preferences, along with its contribution to overall weight, underscores the need for improvement.

Design Implications

The prototyping phase should prioritize increased adjustability, while keeping the bolster system's complexity low by minimizing the number of components and achieving seamless integration of the adaptive materials. It aims to utilize the 3D pressure distribution as a guide, intending to create a system capable of bearing high loads in specific areas while minimizing pressure in others.

To achieve this objective, a comprehensive user testing phase is crucial. It's essential to determine the origins of pressure peaks through testing and to establishing a benchmark of performance using the current system.

Additionally, evaluating the performance of the current material layering, particularly in how these materials interact with the skin's contact patch, is necessary. Long-term effects of fatigue and muscle activity should also be considered, as they significantly impact vehicle comfort over extended periods. Regarding seating performance, the goal is to avoid pressure peaks to reduce overall discomfort. Achieving this involves enabling adaptability in segments of the system, allowing for loads to distribute loads more evenly. Moving from the current passive system to an active adjustable system should be one of the main goals.

Furthermore, during the prototyping phase, the development of a new comfort model is recommended. This model should specifically focus on pressure distributions within the bolster area, which contrasts with the current models that predominantly consider the entire seat.

Main Takeaways:

- The L460 seat faces challenges including complexity, high component count, and difficulties in repair and maintenance.
- The pneumatic system relies mainly on passive components for pressure distribution, limiting its ability to dynamically adapt to individual body shapes and preferences.
- The system's reliance on heavy hardware contributes to the overall weight of the seat, affecting efficiency.
- The proposed should prioritise safety, adaptability, simplicity, and user comfort.
- Pressure distribution testing needed to identify pressure hotspots around the bolster area using a pressure mat.
- Design implications include increasing adjustability while minimizing complexity, integrating adaptive materials, and conducting comprehensive user testing to optimize comfort and performance.

References

Harte, R., Glynn, L., Rodríguez-Molinero, A., Baker, P., Scharf, T., Quinlan, L. R., & ÓLaighin, G. (2017). A Human-Centered Design Methodology to enhance the usability, human factors, and user experience of connected health systems: a Three-Phase methodology. JMIR Human Factors, 4(1), e8. https://doi.org/10.2196/humanfactors.5443

Daffner, R. (2021). The Good, The Bad, And The Complicated. Oliver Wyman. https://www.oliverwyman.com/our-expertise/insights/2021/aug/dealing-with-car-complexity.html

ETD - Technical Trading - SAE J826 H-POINT-MANIKIN - ATD Crash-Test-Dummies. (n.d.). http://www.sae-j826.com/uk/uk_k02_hp_manikin.html

Farah, M. (2019, June 11). Behold, Mercedes has created the world's greatest seat. The Drive. https://www.thedrive.com/article/5514/behold-mercedes-has-created-the-worlds-greatest-seat

Mergl, C., Klendauer, M., Mangen, C., & Bubb, H. (2005). Predicting long term riding comfort in cars by contact forces between human and seat. SAE Technical Paper Series. https://doi.org/10.4271/2005-01-2690

Kolich, M. (2003). Automobile seat comfort: occupant preferences vs. anthropometric accommodation. Applied Ergonomics, 34(2), 177–184. https://doi.org/10.1016/s0003-6870(02)00142-4

Kong YU, Kim DM, Lee KS, Jung MC, 2012. Comparison of comfort, discomfort, and continuum ratings of force levels and hand regions during gripping exertions, Applied Ergonomics 43: 283–289.

Le, P., et al. (2014). "Objective classification of vehicle seat discomfort." Ergonomics 57(4): 536-544.

Liamadis, G. (2013). Research on the Evolution of Automotive Interior as a Living Space: Drive-by-Wire Technology and New Spatial Solutions. Aristotle University of Thessaloniki. https://ikee.lib.auth.gr/record/216131

Looze MP de, Kuijt-Evers LFM, Van Dieën JH. 2003. Sitting comfort and discomfort and the relationships with objective measures. Ergonomics 46: 985–997.

Naddeo, A., et al. (2015). "Proposal of a new quantitative method for postural comfort evaluation." International Journal of Industrial Ergonomics 48(Supplement C): 25-35.

P. Reed, M., Saito, M., Kakishima, Y., S. Lee, N., & W. Schneider, L. (1991). An Investigation of Driver Discomfort and Related Seat Design Factors in Extended-Duration Drivi. JOURNAL OF PASSENGER CARS, 100, 130–159. https://www.jstor.org/stable/44632019

Shankleman, J. (2017, July 7). The electric car revolution is accelerating. Bloomberg.com. https://www.bloomberg.com/news/articles/2017-07-06/the-electric-car-revolution-is-accelerating

Van Der Voort, V. B. (2018). Comfortable Side Supports in Automotive Seating [MA Thesis]. Delft University of Technology.

Van Kamp, I. (2012). The influence of car-seat design on its character experience. Applied Ergonomics, 43(2), 329–335. https://doi.org/10.1016/j.apergo.2011.06.008

Wilker, S., Pekruh, T., & Akar, R. (2023). Interior of the Future - Occupant Requirements during Automated Driving. ATZ Worldwide, 125(11), 48–53. https://doi.org/10.1007/s38311-023-1557-0

Xsensor Technology Corporation. (2021). SENSORS LX210:40.64.02 Product Description. http://www.xsensor.de/wp-content/uploads/2015/11/LX210_40_64_02-2560-Sensoren-127mm-Auflösung-Grösse-50x81cm-Messbereich-007-103Ncm2-Anwendung-Sitze_Rollstühle.pdf

Zenk, R., Mergl, C., Härtung, J., & Bubb, H. (2007). Predicting overall seating discomfort based on body area ratings. SAE Technical Paper Series. https://doi.org/10.4271/2007-01-0346

Zhang, L., Helander, M. G., & Drury, C. G. (1996). Identifying factors of comfort and discomfort in sitting. Human Factors, 38(3), 377–389. https://doi.org/10.1518/001872096778701962

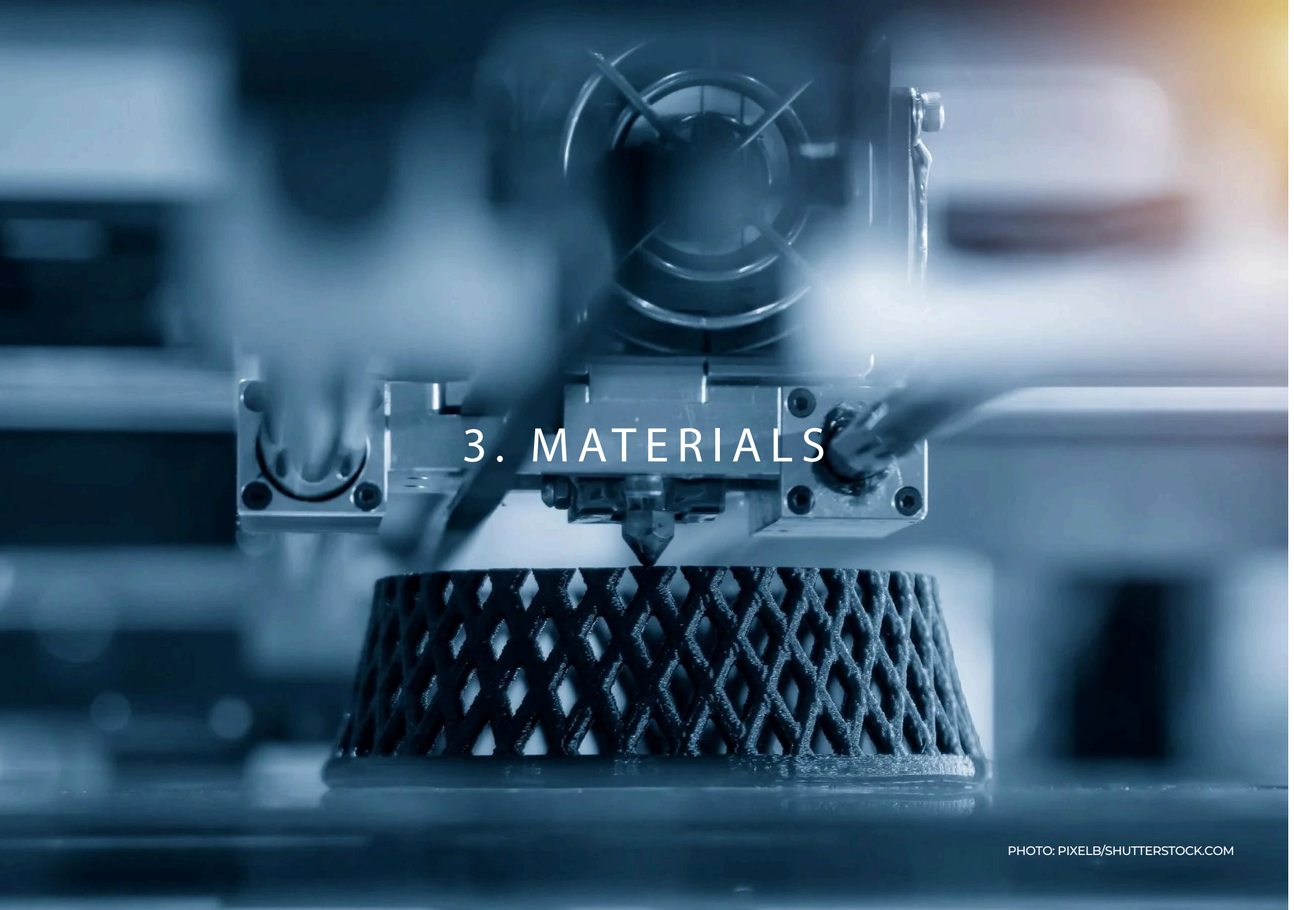

PHOTO: PIXELB/SHUTTERSTOCK.COM

Materials

3.1 Introduction

Shape Memory Materials (SMMs) represent a new category of materials characterized by their capacity to be trained to retain a specific shape (Jani et al., 2014). What sets these materials apart from conventional counterparts is their high sensitivity to external stimuli. In contrast to most materials, which remain passive, SMMs can exhibit active, kinetic, and responsive behaviors under the right conditions.

These materials respond to specific stimuli—such as temperature, electricity, magnetism, humidity, light, pressure, or chemical substances—prompting them to autonomously revert to their predefined shape without human intervention (Bengisu & Ferrara, 2018). For a designer, delving into this field is very fascinating, particularly within the context of car seating. The utilization and exploration of kinetic materials open up a new perspective for examining the mechanical and ergonomic design of bolsters. In contrast to conventional systems that often consist of rigid structures following a limited predefined pattern, SMMs present the opportunity to create a more biomimetic system. Such a system can better correspond to the natural functions of the human body, offering innovative possibilities for enhancing comfort and functionality in car seating design.

Fortunately, extensive research has been undertaken in recent years concerning the development and characteristics of various SMMs, resulting in much readily available information (Bengisu and Ferrara, 2018; Kellaris et al., 2018; Rafiee et al., 202). However, there remains a notable gap in understanding how these materials perform in high-load applications involving direct contact between the human body and an SMM structure, particularly in terms of load distribution—an important topic of this project.

This research aims to provide a comprehensive overview of the landscape of SMMs relevant to this project by research of academic sources as well as physical testing conducted by the author. Moreover, it seeks to delve deeper into understanding the load-bearing capacity of these materials and to determine their relevance in the design of bolsters. By focusing on this aspect, the study aims to contribute valuable insights into using SMMs for optimizing bolster design, especially in scenarios involving substantial loads and human interaction.

3.2 Different kinds of SMM’s

According to Bengisu & Ferrara (2018), three primary groups stand out for prototyping: Shape Memory Alloys, Shape Memory Polymers, and Shape Memory Gels. Sreeram (2023) provided an extensive overview of these materials’ general properties, including their suitability for Property Morphing Catheters (PMC), which also holds relevance for bolster research. This overview, summarized in table 3, guided the initial focus for this research.

	RECOVERY STRESS *in MPa*	VOLUME CHANGE *factor*	STIFFNESS CHANGE *factor*	SPEED *of recovery cycle*	REVERSIBILITY *cycle stability*
SMA *Shape Memory Alloy*	150-300	o	<2	<1s	>1000
SMP *Shape Memory Polymer*	1-3	o	100-1000	<1s - several minutes	10-100
SMG *Shape Memory Gel*	o	100-<1000	100	<1s - 10s	o

TABLE 3: SMA, SMP, SMG CHARACTERISTICS (SREERAM, 2023)

Initially, there was a consideration to involve SMGs in this research. However, due to limited documentation, slow actuation times, and insufficient recovery stress, it was determined that spending efforts elsewhere would be more productive.

In further research, attention shifted to Hydraulically Amplified self-healing electrostatic (HASEL) actuators as a new category of soft actuators capable of mimicking muscle-like functionality. The third section of this chapter explores their mechanisms and assesses their feasibility for design purposes.

3.2.1 Shape Memory Alloy (SMA)

Shape memory alloys (SMAs) are a class of materials that have the ability to “remember” their original shape and return to it after being deformed. These alloys are typically made of metals like nickel, titanium, and copper, or various combinations of these metals.

There are two main categories of Shape Memory Alloys (SMAs): thermal-activated and super elastic alloys (Bengisu & Ferrara, 2018).
Thermal-activated wires retain their deformed shape at room temperature and can be restored to their original shape by applying heat at their activation temperature.

Conversely, super elastic wires naturally revert to their predetermined shape at room temperature.
Additionally, heat-activated wires demonstrate notably higher force capabilities at around ambient temperature of 20C temperature compared to super elastic alloys (Jani et al., 2014).

3.2.1.1 Phases

Shape memory alloys undergo two distinct phases: austenite, and martensite, shown in figure 25 (Rao, 2015).

1. Martensite state is the alloy’s shape at room temperature.
2. Austenite represents the programmed shape above the activation temperature.
3. Annealing serves as the crucial “programming” process.

The annealing process, responsible for setting the shape, occurs at approximately 500 degrees Celsius (Sun & Huang, 2009).

SMA will allow for 5-8% recovery strain in the Austenite phase, deformed (“loaded”) in the Martensite Phase (Rao, 2015).

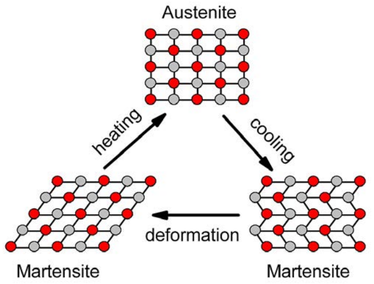

FIGURE 25: DIFFERENT PHASES OF SMA

3.2.1.2 External stimuli & Response Time

SMA can be activated through direct heating (applying heat from the outside), or joule-heating (applying heat through electric current).
Activation ranges (depending on the material) are from 30C to around 130C (Sun & Huang, 2009).

The speed of SMA actuation response relies on factors like shape, size, composition, and the heating method employed.

Heating can prompt a response in less than a second. Utilizing joule heating, higher currents induce quicker temperature changes and, consequently, faster response times. Cooling, however, is typically slower due to the lack of active cooling components in most applications.

Figure 26 shows 2 springs of the same size with 1.0mm diameter left and 1.2mm diameter right, the response times when placed in 65C water were 3.28s and 4.93s respectively. This phenomenon is also explained in research by Tak et al. (2011) (figure 27), where different reaction times and loads were shown for multiple SMA wire diameters.

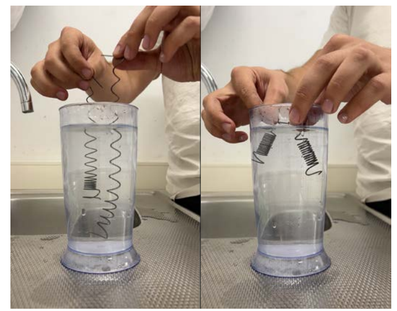

FIGURE 26: REACTION TESTING OF SMA SPRING (NIJHUIS, 2023)

SMAs set to activate at a certain temperature tend to cool more rapidly. This is because of the greater temperature contrast between the transition temperature and room temperature, facilitating a swifter cooling response.

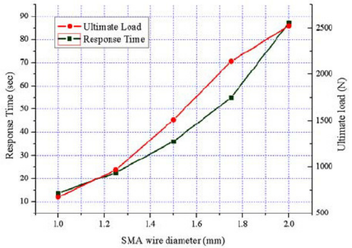

FIGURE 27: LOAD VS WIRE DIAMETER (TAK ET AL. 2011)

3.2.1.3 Types of Activation

One-way actuation involves shaping the material to a specific form during the annealing process. Once the activation temperature is reached, the material consistently reverts to this preset shape. This method, while common, does have limitations in its applications, as it needs external forces to go back to its previous shape (Sun & Huang, 2009).

In contrast, two-way actuation incorporates two shapes: one at high temperature and another at low temperature. However, challenges such as strain deterioration at higher temperatures, tension-compression asymmetry, and reduced strain production limit the commercial feasibility of this method.
Moreover, acquiring two-way activatable materials is considerably more challenging compared to obtaining one-way SMAs due to their limited commercial availability.

One-way actuation seems not suitable for application in repeated actuation of a shape, because the wire does not go back to its original shape when cooled down. Interestingly however, two-way actuation can be achieved using one-way SMAs by combining SMA wire and bias wire, each with opposing shape memory effects (figure 28). These wires work in opposite directions to enable two-way actuation. As described by Sun et al. (2012) “The active elements can be shape memory materials, while the passive element is the substrate in which the active materials are embedded”. This leaves possibilities to use one-way activated materials, with integration of smaller segments to achieve repeated actuation.

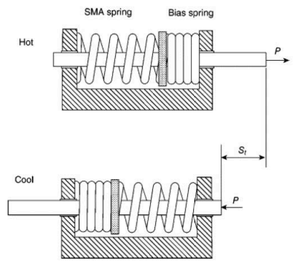

FIGURE 28: BIAS SPRING MECHANISM (NGUYEN ET AL. 2018)

Example and upscaling

A comparable bias-spring mechanism is employed in the valve packs of the massage feature within the L460 seat. Figure 29 illustrates the valve comprising an extremely thin (0.1mm) SMA wire alongside a non-superelastic bias spring At 0.13 Amps and 12.6V the reaction time is almost instant at 0.2s.

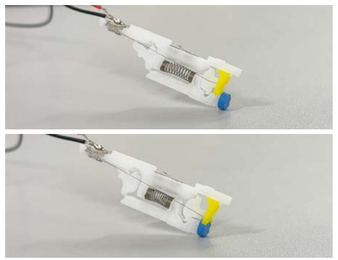

FIGURE 29: SMA ACTUATED VALVE

The challenge arises when attempting to scale up the structure while utilizing SMAs in design. Precisely determining the forces exerted by the SMA wire during shape transitioning becomes notably challenging. Moreover, as the system scales up, both activation and cooling times increase.

Similar activation behavior in the larger structure as observed in the small SMA actuator could not be achieved. Instead, a spring-driven system appeared more feasible for accomplishing the activation (figure 30). Further experimentation and explanation for this phenomenon is done in section 3.2.1.4.

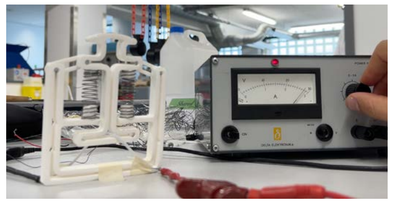

FIGURE 30: UPSCALED SMA ACTUATOR

Superelasticity

Finally, the third category of SMAs is Superelastic Alloys (SEA). These SMAs demonstrate characteristics similar to springs, allowing them to recover up to 8% of their initial elastic deformation. For comparison, standard steel springs typically recover only around 0.5% of their deformation.

Remarkably, SEAs can regain their original shape without requiring heating or cooling. This ability stems from their phase-changing nature under stress, where the transformation reverses once the stress is released.

3.2.1.4 Recovery Stresses and Load Bearing

At room temperature, SMAs are easy to deform but exert considerably higher force during shape recovery. The stress during deformation typically ranges from 50 to 200 MPa, while the stress during recovery spans from 150 to 300 MPa (Rodrigue et al. 2017). Additionally these materials can endure thousands of cycles of shape recovery before degradation occurs.

Notably, in the austenite phase, SMAs exhibit a stiffness approximately twice as high as in their martensite phase. Activation further enhances their stiffness, with an elastic modulus reaching 70 GPa in the activated state and dropping to as low as 40 GPa in the martensite state (Sherif & Ozbulut, 2017).

Research conducted by Rodrigue et al. (2017) gives insights into the trade-offs between stress and strain when utilizing SMA wires versus SMA springs. (figure 31).

The findings highlight the benefits of transforming an SMA wire into a single or double coil spring, significantly increasing displacement by 200% to 1000%. However, this transformation also reduces the maximum force that the material can exert. This insight is crucial to consider when designing a new bolster system, since variations in load exerted by the occupant on the system can be large.

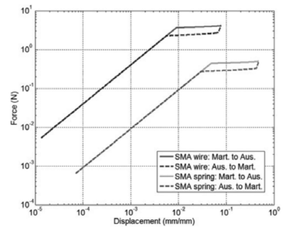

FIGURE 31: WIRE/COIL BEHAVIOUR (RODRIGUE ET AL, 2017)

3.2.1.5 Feasibility for Design

At the Industrial Design Engineering (IDE) faculty, the utilization of SMAs have gained significant popularity. The dedicated workspace and the abundance of available knowledge make SMAs relatively accessible for prototyping purposes.

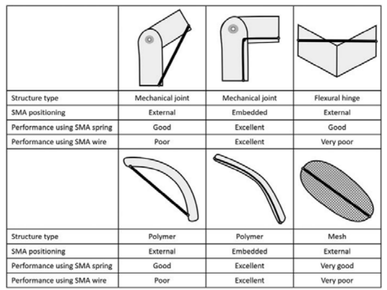

Structure type	Mechanical joint	Mechanical joint	Flexural hinge
SMA positioning	External	Embedded	External
Performance using SMA spring	Good	Excellent	Good
Performance using SMA wire	Poor	Excellent	Very poor
Structure type	Polymer	Polymer	Mesh
SMA positioning	External	Embedded	External
Performance using SMA spring	Good	Excellent	Very good
Performance using SMA wire	Poor	Excellent	Very poor

FIGURE 32: SMA ACTUATORS (RODRIGUE ET AL. 2017)

Among all Shape Memory Materials, SMAs have garnered the most attention. Extensive research, such as the comprehensive study conducted by Rodrigue et al. (2017) on SMA actuators, illustrates the diverse benefits offered by various types of actuators within this category (figure 32). Furthermore, the material's cost-effectiveness and good availability contribute to its appeal and ease of use in various applications. One of the challenges associated with using SMAs is their inherent one-way nature, necessitating additional structures to accomplish two-way designs. This characteristic can pose difficulties and complexities, particularly in applications related to bolstering. Additionally, the relative low load-bearing capacity of SMAs can further complicate efforts to replicate the functionality of a pneumatic system.

Lastly, the shape recovery nature of SMA is based upon adding external energy to reach the shape recovery effect. This means that increased stiffness is only achieved when continuous flow of energy is applied. Testing this with an SMA wire and a cup of brass loads, when the heat was removed, the coil could not hold the load (figure 33).

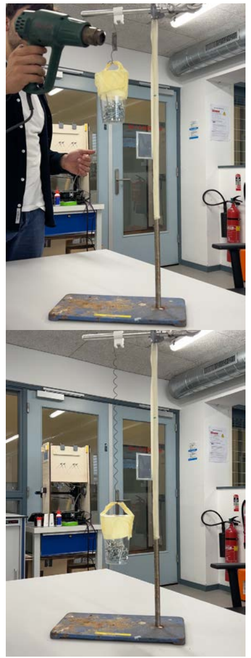

FIGURE 33: REMOVING THE ENERGY SOURCE

3.2.2 Shape Memory Polymers (SMP)

SMPs offer greater design flexibility compared to SMAs while also being more cost-effective. Their primary advantage over SMAs lies in their lower material densities, higher strains (exceeding 400% compared to SMA's 8%), easier shaping, and simpler manufacturing processes due to lower temperatures and pressures (Bengisu & Ferrara, 2018). It's noteworthy that almost any polymer can be transformed into a SMP through physical or chemical crosslinking (Huang et al., 2012).

Crosslinking, the process of bonding polymer chains, can occur through chemical or physical means. Chemical crosslinking involves covalent bonds at the molecular level, while physical crosslinks rely on weaker interactions like coordination bonding, hydrogen bonding, ionic interactions, and van der Waals forces. However, it's important to note that physical bonds generally exhibit lower durability compared to chemical cross-links, making them mechanically and thermally unstable (Arora et al., 2017). The availability and versatiliy of crosslinking techniques greatly expands the range of available materials and and their independent properties when using SMPs.

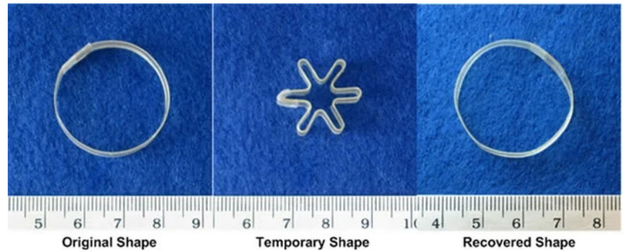

FIGURE 34: SMP SHAPING (SHAPE ART, 2014)

SMPs typically exhibit a two-phase structure consisting of a fixed phase and a reversible phase. The glass transition temperature differs between these phases, being higher in the fixed phase and lower in the reversible phase, allowing for their distinct functionalities.

3.2.2.1 Stimuli

In stress-free conditions, SMPs exhibit the ability to revert to their original shape through various actuation methods, including thermal, electric, magnetic stimuli, exposure to light, and even changes in pH. Among these, thermal activation stands out as the most prevalent method (Wang et al., 2020).

Specifically, thermal activation represents the most commonly employed approach for activating SMPs. This process relies on reaching the material's glass transition temperature (Tg), typically around 60°C, to trigger the shape recovery mechanism.

3.2.2.2 Response time

The response times of Shape Memory Polymers (SMPs) vary depending on the material, with durations ranging from less than a second to several minutes. This variability is influenced by factors such as the conductivity of the material,

its thickness, shape, as well as the temperature. Notably, SMPs tend to be slower in actuation times than SMAs due to their lower thermal conductivity and longer cooling time.

3.2.2.3 Shape recovery behavior of SMPs

The most common shape recovery effect of SMPs is the dual shape memory effect, characterized by a permanent shape and a temporary shape. The temporary shape is achieved from a deformation of the permanent shape induced by an external force. Resetting to the original configuration is triggered by the appropriate stimulus. In this process, the crosslink functions as an element for storing elastic energy during the programming phase and propels the shape recovery during the subsequent recovery stage (Zhou & Huang, 2015).

Conventional SMPs typically exhibit one-way recovery capabilities, enabling them to revert from a deformed state back to their original shape.
When assessing the mechanical properties of SMPs, two perspectives are often considered: the thermo-elastic model and the viscoelastic model.

The thermoelastic model highlights that SMPs behave as elastic materials, experiencing a reduction in stiffness as temperature rises (resulting in a decrease in modulus). On the other hand, the viscoelastic model incorporates stress relaxation, which involves the molecular process of chain sliding when the material is under load, leading to a gradual reduction in stiffness over time (Viscoelastic Properties of Polymers, 2018). The extent of chain slippage can be experimentally determined through a series of time-dependent tests conducted at various temperatures or via dynamic mechanical analysis.

Dual state mechanism

When a SMP is heated above its transition temperature (Ttrans - either Tg or Tm), it becomes pliable and can be reshaped into a new configuration through plastic deformation. Subsequently, upon cooling below Ttrans, the SMP solidifies, preserving the newly shaped form, resulting in a rigid structure.
However, upon heating the SMP again above its transition temperature, it regains its pliability and undergoes a return to its original, initial shape. This cycle illustrates the reversible nature of SMPs, allowing them to transition between temporary and permanent shapes based on temperature alterations above or below their transition temperature) (Wang et al., 2020)).

Orignal shape (from casting) --> Heating --> New shape --> Cooling --> Temporary Shape --> Heating --> Original Shape

Dual component mechanism

This mechanism involves a configuration of two segments. One of these segments must possess a high softening temperature. Reaching Ttrans has the capability to toggle the material's state from rigid to pliable within the operational temperature range.
As described by Bengisu & Ferrara (2018) this setup allows the polymer to undergo plastic shaping when the temperature exceeds Ttrans, engaging the softened state of the material. As the temperature descends below Ttrans, the structure becomes stabilized, effectively fixing the temporary shape.

3.2.2.4 Variable stiffness and Load bearing

The Youngs modulus below Tg and above Tg range from to 0.01 – 3 GPa to 0.001 GPa, respectively. SMPs stiffness decreases when temperature increases, as opposed to SMA which get stiffer (Rafiee et al., 2021).
The general low load bearing capacity for different states of SMP is also confirmed in research by Takashima et al. (2017) (figure 35).

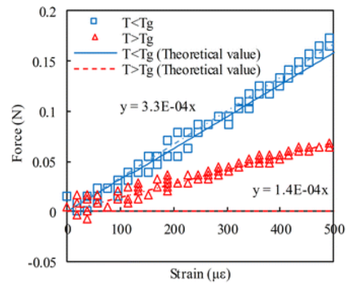

FIGURE 35: FORCE-STRAIN BEHAVIOUR SMP (TAKASHIMA ET AL. (2017)

3.2.2.5. Feasibility for design

Low mechanical and recovery stress of SMP limit their application. In respect to Bolster usage, SMAs have better strength, higher stiffnes, actuation forces and faster actuation times compared to SMPs. To improve mechanical properties, SMPs are often integrated with particles, short fibers and continuous fibers. Especially these continuous fibers increase mechanical strength and stiffness (Jani et al., 2014). They also offer better durability and fatigue performance (Lan et al., 2009). Polyurethane easily commercially available SMP, but temperature needed to utilize morphing behaviour is very high and a cooling mechanism must be included.

Polyurethanes are amongst the most studied SMPs. The material can be made to have shape recovery around room temperature, which is favourable for most designs in the car interior context. These SMPs also allow for a variety of production processes.

As a final input source, Professor Kaspar Jansen, an expert in emerging materials who has worked on projects involving variable stiffness structural joints, was consulted to gather his insights on SMP feasibility for this project.

His project was on developing an SMPC structural joint for adaptable buildings, allowing changes in stiffness and shape. These structures promise up to 70% energy savings compared to traditional ones.

He explained that when polymers reach their glass transition temperature (Tg), they excel at damping vibrations. However, Tg isn't a fixed value but rather a range. Excessive heating can lead to strains slipping excessively. Therefore, regarding systems where bolsters must handle shape change and vibrations (similar to polymer/aramide joints), he recommends against using polymers. He points out the absence of a shape-shifting effect, only damping, which might not suffice for a comfortable experience.

3.3 HASELS

Soft robotics have faced limitations with current actuator such as insufficient power, slow speeds, inefficiency, and fragility. HASEL actuators address these challenges in a different way from conventional SMMs. HASELS blend electrostatic and hydraulic to mirror nature's adaptability, which makes them interesting to use in a system that handles the contours of the human body (figure 36).

The current bolster design demands a system to be capable of executing repetitive tasks consistently without deterioration. These systems require responsiveness in about 8s (as explained in section 2.2.3), high load-bearing capacity, and long-lasting durability. As previously highlighted, choosing any type of shape-memory material invariably entails compromising one or more of these attributes.

HASEL actuators generate hydraulic pressure using electrostatic forces acting on a liquid dielectrics within a Poly Propylene (PP) bag. They offer strength, flexibility and self-healing capabilities all at a fast response time (up to 60hz).

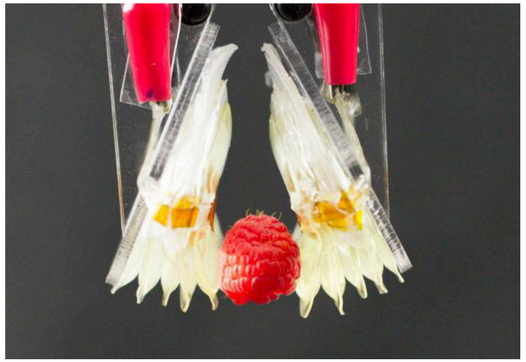

FIGURE 36: HASEL ACTUATOR (UNIVERSITY OF COLORADO (2018)

The technology is relatively novel and therefore the application of them in car seating is relatively unexplored. One major challenge is the high voltage they demand in operation (between 5kV and 10 kV) to create the Maxwell stresses that cause hydraulic pressure to build.

This section explains the main principle of HASELs and evaluates their suitability for design.

3.3.2 Working Principle

According to Acome et al. (2018), the core principle behind HASELs involves applying an electric field across two electrodes—one positive and one negative—positioned on a flexible shell containing a dielectric fluid. This setup generates Maxwell Forces. Visualizing these forces, can be compared to the effect of filling a silicone bag two-thirds full with olive oil and then applying pressure to one side: the oil will accumulate on the side without pressure, causing the bag to contract in length while expanding in height (figure 37 & 38). This effect occurs due to the incompressibility of the liquid and inextensibility of the shell.
When the electric current is taken off, the fluid should spread across the full surface of the shell evenly. To achieve this precision in shaping in fabrication is essential.

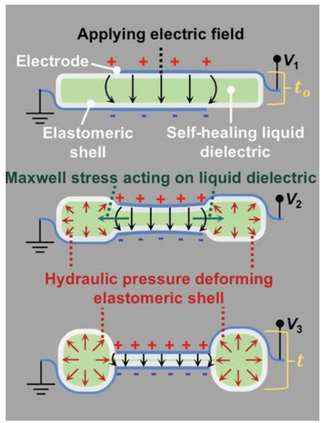

FIGURE 37: HASEL WORKIG PRINCIPLE (ACOME ET AL. 2018)

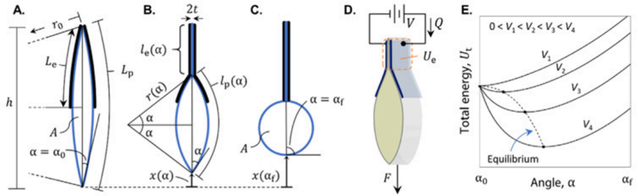

FIGURE 38: HASEL SIZING (KELLARIS ET AL. 2018)

3.3.3 Response Time

HASEL Actuators are known for their quick response and linear contraction on activation.
A study by Kellaris et al. (2018) has shown that linear contraction of 10% can be achieved for a bandwith up to 50 Hertz. Higher frequencies showed deterioration of contraction force and strain.

3.3.4 Load bearing capacity

In another study by Kellaris et al. (2018) they conducted thorough research into the load-bearing capacity of HASELs and explored the impact of various design parameters.

The study presents the normalized scaling behavior across different lengths and widths of HASEL actuators, at different operation voltages (figure 39).

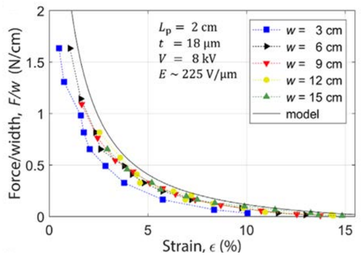

FIGURE 39: FORCE/STRAIN BEHAVIOR HASELS (KELLARIS ET AL. 2018)

The graph reveals a notable trend: the actuation force diminishes as strains increase, reminiscent of behaviours observed in SMAs. Additionally, it highlights that the width of the cell has minimal influence on the relative performance of the actuators. Higher voltage means higher force at lower strain.

When looking further into how the study optimized the performance of the actuators, interestingly it can be seen that by lowering pouch length Lp (image X), mass of the actuator is quadratically lowered (because of lower crosssection), but no force-strain deterioration takes place. This means that multiple smaller actuators can achieve the same performance as one large actuator at a reduced mass. Note that scaling down does have a limit due to limited flexibility and thickness of the shell.

3.3.5 Feasibility

Apart from the high voltage needed to operate HASELs at the desired Maxwell stresses, most components to produce the actuators are readily available:

- 20 micron BOPP Sheet available for order online.
- 50 cst silicone oil available at art supply store.
- Copper tape and conductive paint at IDE.

(Mitchell et al., 2019).

When shaping and producing the actuators, an important aspect is the forming of the BOPP shell. During testing (appendix X) I found that using a heat press with CNC's components worked best to seal two layers of BOPP together while leaving an opening for a syringe with silicone fluid.

On the power supply side there is assistance available from Dr. M. Ghaffarian Niasar at the High Voltage Lab at the faculty of electrical engineering. Together with him the aim is to test the shape effect, load capacity, strain difference and actuation time of multiple actuators.

This is done to get a proof of concept and evaluate whether the HASELs are suitable for operation in a car seat bolster.

3.4 HASEL- vs SMA Actuators

3.4.1 Introduction

As outlined in section 3.1.3, the approach of this project involves a modified version of the Material Driven Design Method. Prior to delving into the ideation phase of the conceptualization, it is necessary to select a singular shape-morphing material that will serve as the foundation for the actuation of the adjustable system. While both Shape Memory Alloy (SMA) and HASEL materials have been explored in the literature, a considerable amount of time has initially been dedicated to the "tinkering" phase with SMA.

To ensure a fair comparison between the two materials, extensive efforts have been invested in creating testable HASEL prototypes. The details of this process are shown in appendix X, and the findings from these efforts are utilized in this section to assess the viability of both materials for this project.

Shape Control

HASEL actuators provide extensive shape control capabilities, allowing for the production of completed shapes or partial shapes that can be combined. This flexibility extends to 3D control of the shapes (Kellaris et al., 2019). When coupled with a suitable power supply and control system, these actuators exhibit rapid actuation times, often falling below 1 second and reaching frequencies of up to 50Hz.

SMA-based actuators similarly provide a diverse range of achievable shapes. However, achieving a desired shape while managing the corresponding load requires consideration of wire or shape geometry. This geometry significantly influences both the power required to activate the system and also influences the design of the bias mechanism. In contrast, HASEL actuators exhibit high relative loads and fast actuation across various sizes within similar ranges, mitigating the impact of these factors to a considerable extent.

Power Consumption

While HASEL actuators require very high voltage supplies to generate appropriate Maxwell stresses, their current demand remains quite low. Many actuators documented in the literature set a current limit at 1 milliamp to prevent electrostatic discharge (Morton, 2022). With an operational voltage of 7kV, as specified in section 3.3 of this report, the total power consumption can be calculated as 8kV * 1mA = 8W (P=V*A). On the other hand, SMA requires lower voltages but higher currents. For a 0.381mm diameter SMA wire, the current demand for reaching activation temperature would be around 2.7A at 12.7V, resulting in a power consumption of 12.7V * 2.7A = 34.3W.

Both methods require a consistent power supply to enable shape morphing behavior, posing a similar design challenge. Although the overall power consumption of HASEL is lower than that of SMA, the demand for a 7kV power supply presents other challenges for use in a car seat bolster, such as safety and the car architecture providing enough voltage to reach the demand.

Feasibility

Regarding component and material availability, the components for HASELs were somewhat easier to obtain due to the relatively common materials they consist of. During testing with both materials, SMA proved to be very accessible for producing functional prototypes, as demonstrated in section 3.2.1.5, making it relatively easy to experiment with.

In contrast, HASEL actuators seemed straightforward initially but posed significant challenges in creating a fluid pouch with a leak-free seal. The process of creating the pouch are shown in figure 54. Out of the 19 prototypes manufactured, only 2 successfully survived for testing (figure 53).

During testing, it became apparent that careful consideration of symmetry in pouch design and electrode placement is crucial to achieve the intended shape-shifting effect, or any movement at all, with HASEL actuators. In contrast, SMA demonstrated more promising results in this regard, allowing for easier actuation and faster prototyping

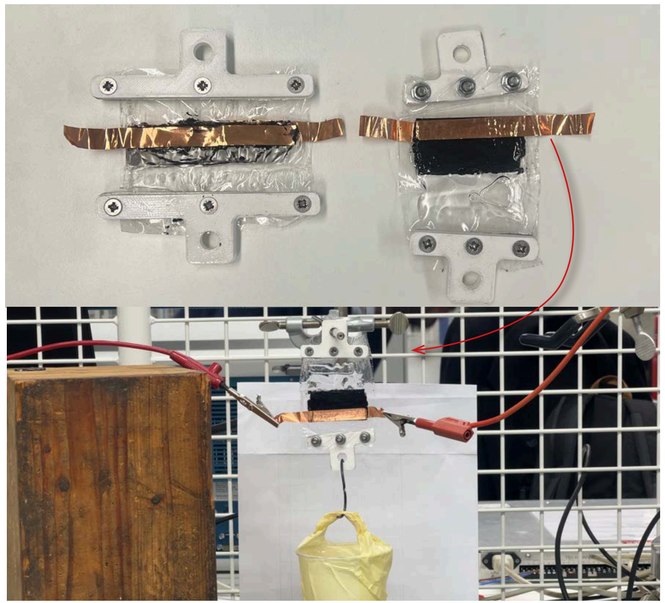

FIGURE 53: HASEL ACTUATORS BEFORE AND DURING TESTING

Safety

Due to HASELs relying on a thin layer of film as an enclosure for the liquid inside the pouch and operate at high voltages, they are vulnerable to dielectric breakdown, posing a significant risk of fire (Kellaris et al., 2019).
In contrast, SMA requires higher amps, which theoretically are considered more hazardous to humans than higher voltages. However, because the active element of SMA actuators, like copper wires, can be isolated from human contact, SMA is deemed safer than HASEL.

Sustainability

One of the key advantages of SMA is that once a wire loses its shape-morphing capacity, it can almost always be retrained to perform as initially intended (Jani et al., 2014). This aspect presents an interesting proposition in terms of sustainability.

On the other hand, HASEL appears to be more one-time-use oriented, as indicated by the literature provided in section 3.3. The pouches are prone to leakage and typically need to be replaced entirely afterward. Additionally, the Silicone Gel used as a dielectric is vulnerable to leakage, potentially contaminating the surroundings. Both the liquid and the PP bag, which may be contaminated by the gel, have limited end-of-life applications i.e. degradation in quality of the material (Krosofsky & Krosofsky, 2021).

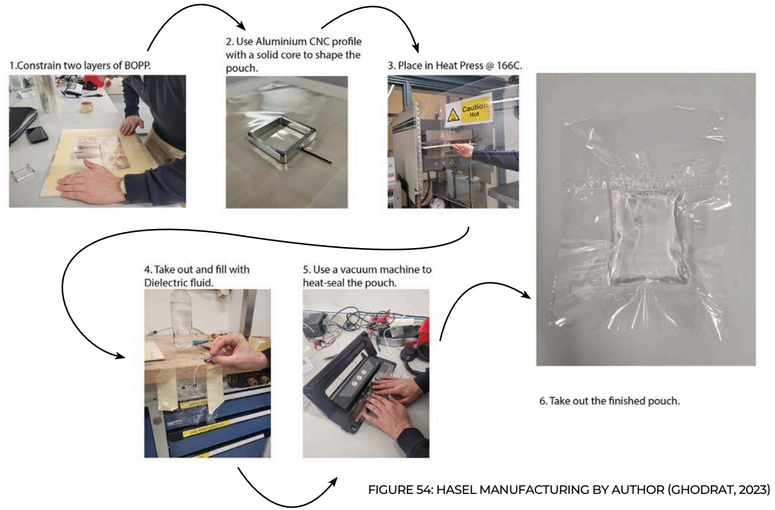

FIGURE 54: HASEL MANUFACTURING BY AUTHOR (GHODRAT, 2023)

	Shape Control	Feasibility	Power	Safety	Sustainability	Shape Control
HASEL	● ●	●	●	● ●	●	
SMA	●	● ●	●	●	● ●	

TABLE 4: ADVANTAGES AND DISADVANTAGES OF BOTH ACTUATORS.(NIJHUIS, 2024)

Conclusion

The advantages of both HASEL and SMA actuators are outlined in table 4.

The “Harris Profile” evaluation method is used as a visual representation of the strengths and weaknesses of both systems. Based on this visualization, a decision can be reached regarding which material is most suited for further exploration. The Harris profiles for both materials are depicted in Figure 54.

This method involves considerations not only of the performance of the materials but also is based on the designer’s intuition, drawing from the cumulative knowledge acquired throughout the project.

After weighing the Harris profiles and considering the general applications of the different types of actuators, the decision has been made to design the adjustable bolster system based on a shape memory alloy actuated system.

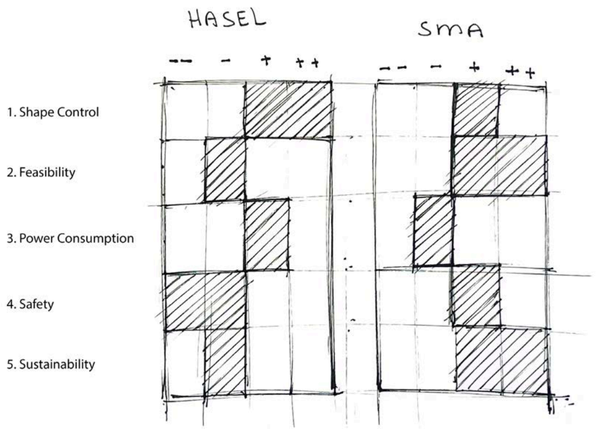

FIGURE 55: HARRIS PROFILES FOR BOTH MATERIALS (NIJHUIS, 2024)

Main Takeaways

- SMMs can have specific shapes and retrun to predefined shapes in response to stimuli like temperature or electricity, offering innovative possibilities for car seating design
- SMAs can be activated through direct heating or joule-heating, and their response time depends on various factors such as shape, size, composition, and heating method.
- SMAs undergo phases (austenite, and martensite), with varying response times and load-bearing capacities.
- SMPs have dual shape memory effects, allowing them to revert from a deformation at high temperatures back to their original shape. They also have a variable stiffness and load-bearing capacity depending on temperature, but is generally very low.
- While HASEL actuators require high voltage for operation, most components are readily available, and load bearing capacity seems very good.

References

Acome, E., Mitchell, S. K., Morrissey, T. G., Emmett, M. B., Benjamin, C., King, M. E., Radakovitz, M., & Keplinger, C. (2018). Hydraulically amplified self-healing electrostatic actuators with muscle-like performance. Science, 359(6371), 61–65. https://doi.org/10.1126/science.aao6139

Arora, B., Tandon, R. P., Attri, P., & Bhatia, R. (2017). Chemical crosslinking: Role in protein and peptide science. Current Protein & Peptide Science, 18(9). https://doi.org/10.2174/1389203717666160724202806

Bengisu, M., & Ferrara, M. (2018). Materials that Move. In SpringerBriefs in applied sciences and technology. https://doi.org/10.1007/978-3-319-76889-2

Duff, M. (2022, April 7). 2022 Range Rover (L460) | PH Review. PistonHeads UK. https://www.pistonheads.com/news/ph-driven/2022-range-rover-l460--ph-review/45534

Ferry, J. D. (1961). Viscoelastic properties of polymers. Journal of the Electrochemical Society, 108(7), 142C. https://doi.org/10.1149/1.2428174

Huang, W., Zhao, Y., Wang, C. C., Ding, Z., Purnawali, H., Tang, C., & Zhang, J. L. (2012). Thermo/chemo-responsive shape memory effect in polymers: a sketch of working mechanisms, fundamentals and optimization. Journal of Polymer Research, 19(9). https://doi.org/10.1007/s10965-012-9952-z

Jani, J. M., Leary, M., Subic, A., & Gibson, M. (2014). A review of shape memory alloy research, applications and opportunities. Materials in Engineering, 56, 1078–1113. https://doi.org/10.1016/j.matdes.2013.11.084

Karana, E., Barati, B., Rognoli, V., & Van Der Laan, A. Z. (2015). Material Driven design (MDD): a method to design for material experiences. International Journal of Design, 9(2), 35–54. http://repository.tudelft.nl/islandora/object/uuid:7359026d-57f5-4f63-9835-126c5d23baed/?collection=research

Kellaris, N., Venkata, V. G., Smith, G. M., Mitchell, S. K., & Keplinger, C. (2018). Peano-HASEL actuators: Muscle-mimetic, electrohydraulic transducers that linearly contract on activation. Science Robotics, 3(14). https://doi.org/10.1126/scirobotics.aar3276

Lan, X., Liu, Y., Lv, H., Wang, X., Leng, J., & Du, S. (2009). Fiber reinforced shape-memory polymer composite and its application in a deployable hinge. Smart Materials and Structures, 18(2), 024002. https://doi.org/10.1088/0964-1726/18/2/024002

Mitchell, S. K., Wang, X., Acome, E., Martin, T., Ly, K., Kellaris, N., Venkata, V. G., & Keplinger, C. (2019). An Easy-to-Implement toolkit to create versatile and High-Performance HASEL actuators for untethered soft robots. Advanced Science, 6(14). https://doi.org/10.1002/advs.201900178

Morton, A. (2022, January 31). Electrical Safety with High Voltage Actuators. Artimus Robotics. https://www.artimusrobotics.com/post/safety-with-high-voltage-actuators

Rafiee, M. M., Baniassadi, M., Wang, K., Baniasadi, M., & Baghani, M. (2021). Mechanical properties improvement of shape memory polymers by designing the microstructure of multi-phase heterogeneous materials. Computational Materials Science, 196, 110523. https://doi.org/10.1016/j.commatsci.2021.110523

Rao, A. (2015). Design of Shape Memory Alloy (SMA) actuators. In SpringerBriefs in applied sciences and technology. https://doi.org/10.1007/978-3-319-03188-0

Rodrigue, H., Wang, W., Han, M. W., Kim, T. J. Y., & Ahn, S. (2017). An overview of shape memory Alloy-Coupled actuators and robots. Soft Robotics, 4(1), 3–15. https://doi.org/10.1089/soro.2016.0008

Sherif, M. M., & Ozbulut, O. E. (2017). Tensile and superelastic fatigue characterization of NiTi shape memory cables. Smart Materials and Structures, 27(1), 015007. https://doi.org/10.1088/1361-665x/aa9819

Sun, L., & Huang, W. M. (2009). Nature of the multistage transformation in shape memory alloys upon heating. Metal Science and Heat Treatment, 51(11–12), 573–578. https://doi.org/10.1007/s11041-010-9213-x

Sun, L., Huang, W., Ding, Z., Zhao, Y., Wang, C. C., Purnawali, H., & Tang, C. (2012). Stimulus-responsive shape memory materials: A review. Materials in Engineering, 33, 577–640. https://doi.org/10.1016/j.matdes.2011.04.065

Takashima, K., Kamizono, H., Takenaka, M., & Mukai, T. (2017). Force sensor utilizing stiffness change of shape-memory polymer based on temperature. ROBOMECH Journal, 4(1). https://doi.org/10.1186/s40648-017-0086-2

Tak, W., Lee, M., & Kim, B. K. (2011). Ultimate load and release time controllable non-explosive separation device using a shape memory alloy actuator. Journal of Mechanical Science and Technology, 25(5), 1141–1147. https://doi.org/10.1007/s12206-011-0304-4

Van Boeijen, A., Daalhuizen, J., Van Der Schoor, R., & Zijlstra, J. (n.d.). Delft Design Guide: Design Strategies and Methods. Bis Pub.

Van Der Voort, V. B. (2018). Comfortable Side Supports in Automotive Seating [MA Thesis]. Delft University of Technology.

4. CONCEPTUALISATION

4.1 Introduction

This section of the report explains the progression from literature research to the final prototype. It provides a detailed overview of the steps involved in developing a new side bolster actuation system, explaining the considerations made throughout the process. During the conceptualization phase, the project follows to the basic design cycle as explained by van Boeijen et al. (2010) (Figure 40) and incorporates the “material-driven design” approach, as explained below.

4.1.1 Explanation design cycle

This design cycle commences with an analysis section wherein the conclusions made in the literature research are reviewed and reflected upon. This section delves into exploring how the identified knowledge gap in the literature can be addressed through the integration of shape morphing design and ergonomic principles. Any gaps in information that are identified in this section are addressed through additional research as needed.

Following the analysis, there is a synthesis phase during which an extensive list of criteria and design objectives is formulated. This involves establishing technical and non-technical requirements and defining clear design goals for the ideation and embodiment section of the design. These design goals are rooted in feasibility, complexity, (ergonomic) performance and sustainability of the final concept.

With established goals and potential design directions, the simulation stage commences. Ideation on various concepts begins, with a focus on shape morphing and ergonomic design principles. Drawings and models are created to identify which application of a shape morphing design could be suitable for implementation in the side bolster of the L460 seat.

After ideation, the proposed ideas undergo evaluation against the predetermined design criteria. The most suitable concept is determined using the “Harris Profile” for significant decisions and the “value” method for smaller decisions, both of which will be explained further on in this report.

The concluding stage of the design cycle involves decision-making. Following an evaluation of each proposed idea by using appropriate methodologies for assessment, a decision is made either incorporate the proposal into the prototype or to continue the ideation process.

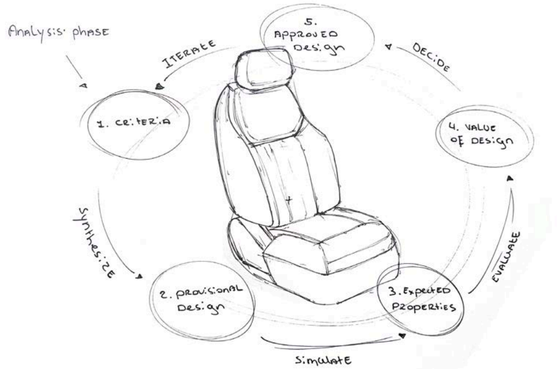

FIGURE 40: THE BASIC DESIGN CYCLE AS EXPLAINED BY VAN BOEIJEN ET AL. (2010)

4.1.2 Cycle within a cycle

The aforementioned design cycle is a dynamic process that can be applied either in its entirety for full prototype development cycles, such as those for a HASEL or SMA-driven bolster system, or smaller loops can be implemented for addressing more modest design challenges, as depicted in figure 41. These smaller loops function as intermediate design evaluations, allowing for quick iterations, ideation, and decision-making based on prior knowledge and common sense, when practical, without the need for a complete cycle. Throughout the development stage of this project, both large and small design cycles are used to reach a final prototype in a consistent and efficient manner.

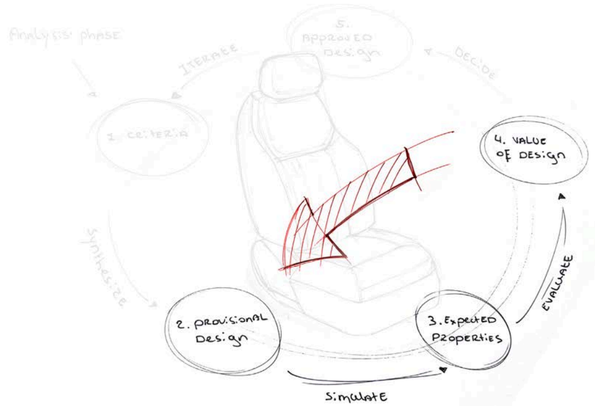

FIGURE 41: THE BASIC DESIGN CYCLE APPLIED IN THIS RESEARCH (NIJHUIS, 2024)

4.1.3 Material driven design

This project, to a certain extent, adopts the method of Material Driven Design (MDD), methodology developed by Karana et al. (2015). This approach enables designers to make meaningful designs with the material serving as the starting point. Described as a method to “create material experiences,” MDD emphasizes on the cognitive aspect of material-driven design, aiming for an experience as outcome rather than a mechanical system, as is the case with this project.

The method consists of four main steps:

1. **Understanding the material: Technical and Experiential Characterization.**
   Achieved through hands-on exploration of the material, user studies, and material benchmarking

2. **Creating Materials Experience Vision.**
   Involves comprehending the material’s characterization and reflecting on its intended purpose.

3. **Manifesting Materials Experience Patterns.**
   Conducted through user studies to bring out patterns in the material’s experiential aspects.

4. **Designing Material/Product Concepts**
   Executed through the creation and testing of prototypes.

Since this project places an emphasis on achieving a mechanical system for bolster adjustability as a primary outcome, rather than solely focusing on the cognitive experience of the user, an adaptation to the original method was implemented, aligning with the basic design cycle described in section 3.1.1 and detailed in Figure 42.

In the adjusted method, the initial two steps remain unchanged, while steps 2 and 3 are modified to better suit the project’s scope.

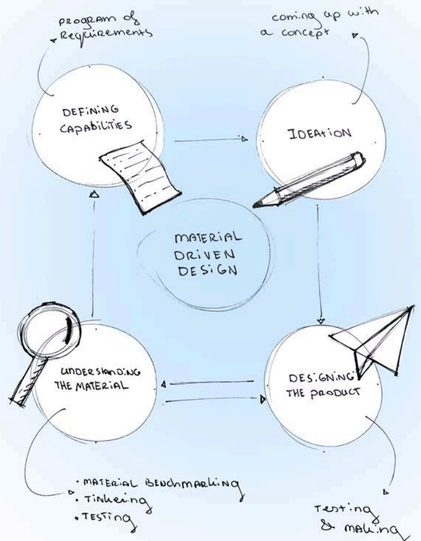

FIGURE 42: THE ADJUSTED DESIGN CYCLE BASED ON THE METHODOLOGY BY KARANA ET AL. (2015)

Step 2 is revised to:

“Defining ergonomic and seating performance”

This entails establishing a comprehensive list of requirements and preferences for the system to adhere to.

Step 3 is revised to:

“Ideation of a morphing material-based adjustable bolster system”

This phase involves brainstorming and conceptualizing of a shape morphing material-based bolster system.

This methodology serves as a guideline to how design decisions are made throughout the basic design cycle within the project. To conclude, most design decision will be made based on their value to the project.

4.1.4 Literature Conclusion & Design Goal

As part of the analysis phase in the design cycle, the insights derived from the literature research will serve as the foundation for developing design goals and system requirements. Both technical and non-technical design goals and requirements are formulated based on these findings. A detailed overview of the program of requirements can be found in appendix C.

Throughout the prototyping phase, each potential design decision is tested for its alignment with these goals and requirements. This testing is done with the use of multiple evaluation methods to assess their value to the overall design. Within the literature research multiple conclusions on the feasibility and performance of multitude of design considerations were made. From these findings, the primary goal can be summarized as:

“Designing an active bolster adjustability system that mitigates discomfort by avoiding peak pressures on the contact patch, while maintaining simplicity in its mechanical design.”

This design goal aims to establish a foundation for creating a product that addresses the knowledge gap identified in the literature research. Specifically, it aims to bridge the existing gap between car bolster ergonomics and the use of shape morphing materials in the design of these bolsters.

4.1.5 Reflection on Literature Findings

In the literature research, several recommendations were made along with findings. These are reassessed here in terms of their relevance to the scope of this project.

Comprehensive user test

Literature recommendation:

Conduct a more thorough user test with the L460 seat and pressure mat to identify peak pressures and their origins.

Project approach:

Given the project's significant reliance on the ergonomic performance of the final system, a more comprehensive user study will be undertaken to investigate pressure distribution on the contact patch of the occupant.

Ergonomic performance evaluation and muscle fatigue study

Literature recommendation:

Evaluate the ergonomic performance of the current material layering and investigate the long-term effects of muscle fatigue.

Project approach:

The decision has been made not to delve deeper into this aspect. Instead, a larger effort will be directed towards developing a proof of concept for the mechanical adjustment system. However, there will be an assessment to determine suitable material layering for implementation in this new design.

New comfort model development

Literature recommendation:

Development of a new comfort model based on the model by Vink and Hallbeck (2012).

Project approach:

Similar to the ergonomic performance evaluation, the decision is to focus efforts on development of the mechanical system. Development of a new method at this stage does not appear evidently relevant.

This reevaluation aligns the project's focus with the most relevant aspects, prioritizing user testing and the development of a proof of concept for the mechanical adjustment system.

Decision for material driven actuator

The material section of the literature report concluded in identifying two key material-actuated principles, namely Shape Memory Alloy and HASEL, as potentially suitable for handling the actuation and shape morphing aspects of the final design. To determine their suitability for the project, these materials need to be evaluated against each other based on the program requirements and their feasibility for the project.

4.2 Pressure Distribution Test

4.2.1 Introduction

4.2.1.1 Objective

The primary objective of this study is to examine the pressure distribution on the car seat bolster when a participant occupies it for a duration of 15 minutes. This timeframe allows for the foam to appropriately settle and conform to the participant's contours (D.Withey, Personal communication, 2023). The study is designed to gain insights into comfort, support, and to identify potential areas of peak pressure.

The goal of the test is to collect quantitative data showing the pressure distribution in N/cm2 on the contact patch of the upper bolster area. Additionally, qualitative insights on seat performance will be gathered through a questionnaire completed by the participants. The quantitative data will be visually represented and used as a benchmark for shaping the final product.

This study aims to serve as a validation or rejection of the findings in section 2.2.5 of this report, and its outcomes will play a role in the development of a prototype, alongside relevant information from existing literature.

4.2.1.2 Participants and Sample size

The study involves a total of 10 adults, consisting of 7 men and 3 women.
All participants provided informed consent (Appendix D) to participate in the experiment. Figure 43 shows the distribution of heights and weights of the participants.
All participants were recruited through invitation at the Industrial Design Engineering faculty at the Delft University of Technology.

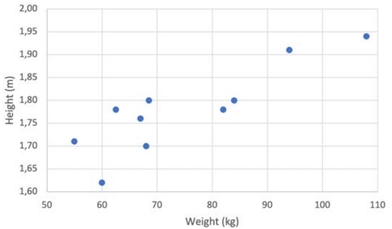

FIGURE 43: WEIGHT AND HEIGHT OF EACH PARTICIPANT

4.2.1.3 Hypothesis

The hypothesis for this study is:

"When a group of users with diverse body sizes occupies a static seat, the combined pressure profile on the bolster will exhibit a significant spread across the contact surface."

The expectation is that there will be no consistent pressure peaks identified that apply to every participant. This anticipated outcome serves to affirm the relevance of an adjustable system, confirming the idea that individualized adjustments are crucial to accommodate the varying pressure distribution patterns among participants.

4.2.1.4 Materials (Figure 44)

1. L460 Seat with Xsensor Pressure Mat
2. Computer with Xsensor V8 Software Scale
3. Timer
4. Informed Consent Form
5. Questionnaire

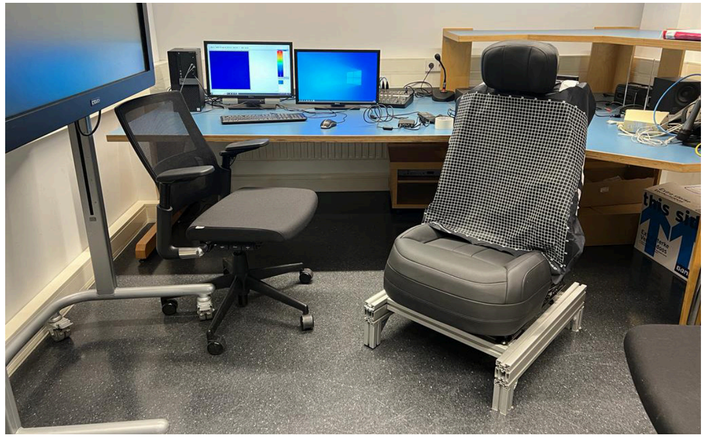

FIGURE 44: THE SETUP FOR THE ERGONOMICS TEST

4.2.1.5 Procedure:

Introduction & informed consent
The study is introduced, and participants are presented with an informed consent form. Participants are requested to sign the form, confirming their understanding of the study's nature and agreement with its contents.

Information collection
Basic participant information, including age, gender, height, and weight, is collected.

Seat preparation
Ensure proper placement of the pressure mat on the seat. Seat and foam are conditioned by allowing them to reach a 21°C ambient temperature overnight. The seat is placed at the appropriate angle to simulate lateral forces on the bolster.

Participant seating
Participants are asked to sit in the seat, and data recording begins. A 15-minute timer is started, and participants are instructed to place their hands on top of their legs (figure 44). Jackets or thick sweaters are to be removed if deemed appropriate.

Observation
Observe during the test if there are any noticeable actions done by the participant that could influence the outcome of the test.

Questionnaire
After the 15-minute period, participants are asked to fill out a questionnaire. They are encouraged to provide qualitative feedback on their overall experience, specifying any observations or discomfort.

End
Participants are thanked for their time and contribution to the study.

4.2.2 Pilot Test

During the pilot test, the participant showed a relatively narrow upper body, and at a seat angle of 4°, the pressure readings on the side bolster were notably low. The decision was made to increase the seat angle to 12°. When retesting at this adjusted angle, the pressure readings on the side bolster became more pronounced.
Based on feedback from the participant, the initial open-ended question (rating 1 to 10) in the questionnaire was modified to a 7-point Likert scale for enhanced clarity.



FIGURE 44: PARTICIPANT DURING THE PILOT TEST

Initially, the measurements were conducted at a frequency of 10Hz, resulting in large file sizes and slow analysis with no substantial benefit. To address this, the measurement frequency was adjusted to 20 readings per minute, or 1/3Hz, to optimize file sizes and improve analysis efficiency.

4.2.3 Test observations & Questionnaire Results

The participants rated the overall comfort of the seat with an average grade of 5, indicating "Slightly Comfortable." Discomfort was consistently mentioned in the middle to upper portion of the right side of the participants' back, near the shoulder.
A recurring observation was that participants found the seating position too upright. This was further confirmed during the test, as participants were observed needing to move their heads forward an unnatural amount, suggesting a potential need for adjustment in the seating position for enhanced comfort.

4.2.4 Data Analysis

The data analysis process involves extracting raw data from XSensor Pro v8 in the form of .txt files, upon which the analysis is then done in Microsoft Excel. These files provide pressure data for each cm2 on the pressure mat, measured at 1/3 Hz over a 15-minute duration.

Upon transferring the .txt data to Excel, a challenge emerged in the data filing structure. Each frame was recorded in a 48x48 grid, separated by multiple rows of logging information. To create a more organized structure for analysis, an Excel VBA macro script was written. This script removed unwanted rows of basic information, resulting in an uninterrupted sequence of 300 frames of 48x48 data points per test. The additional 35 columns of data outside of the cluster that corresponds with the bolster area, named KT1 (figure 48), were manually removed for all tests, leaving 14,400 rows of data per test after the script ran.

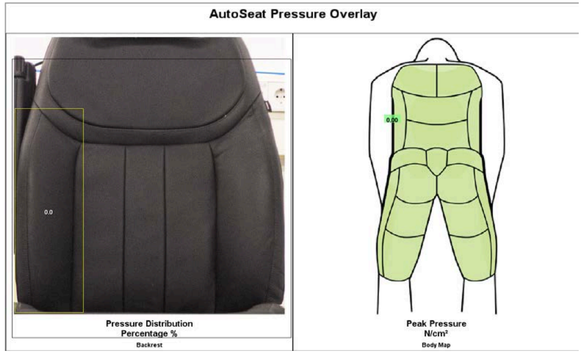

FIGURE 45: THE KT1 CLUSTER SHOWN IN YELLOW ON THE LEFT

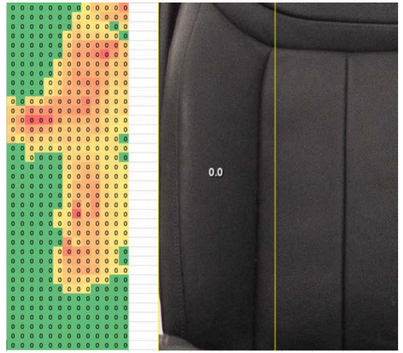

FIGURE 46: ALIGNMENT OF THE GRID WITH THE DATA

Upon transferring the .txt data to Excel, a challenge emerged in the data filing structure. Each frame was recorded in a 48x48 grid, separated by multiple rows of logging information. To create a more organized structure for analysis, an Excel VBA macro script was written. This script removed unwanted rows of basic information, resulting in an uninterrupted sequence of 300 frames of 48x48 data points per test. The additional 35 columns of data outside of the cluster that corresponds with the bolster area, named KT1 (figure x), were manually removed for all tests, leaving 14,400 rows of data per test after the script ran.

Due to limitations in the software, it was not possible to directly export the specific side bolster grid. To address this, adjustments were made in Excel to align with the LX210's 48x48 grid with KT1 (figure 46).

For further analysis, another script was employed to loop through all the rows of data using an "OFFSET" command. This script divided the data into 300 48x13 grids, combining the values to show average and peak pressure (figure 47). Due to the static nature of the test only a minimal noticeable pressure gradient can be observed when plotting pressure-over-time graphics, as shown in figure 48. It was decided not to analyze the pressure gradient

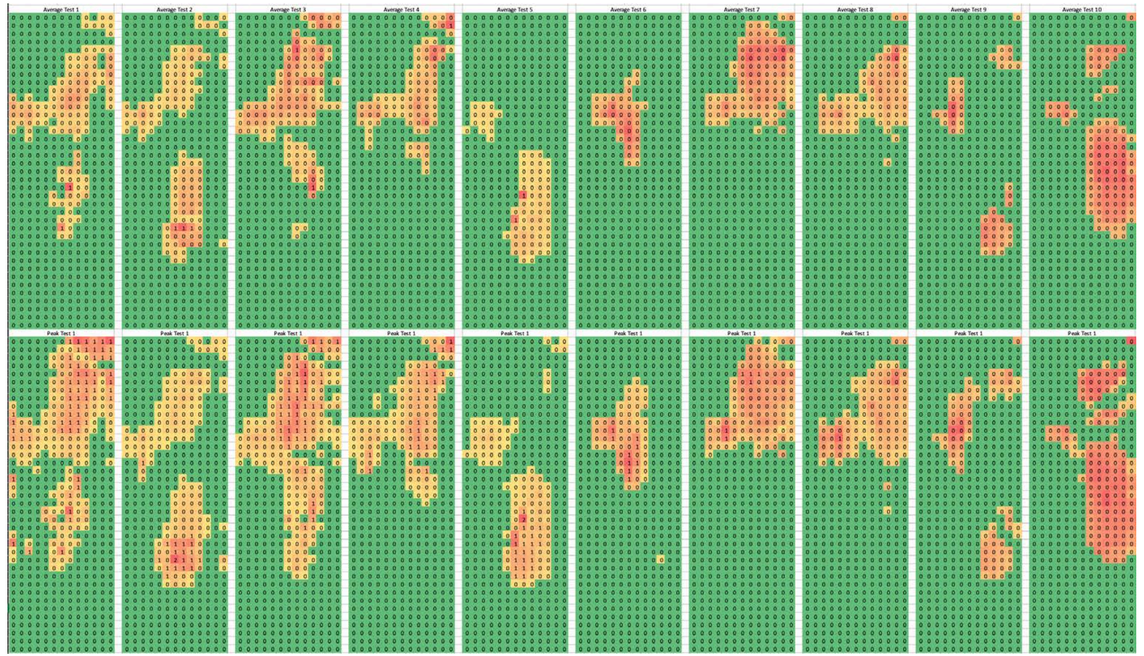

FIGURE 46: ALIGNMENT OF THE GRID WITH THE DATA

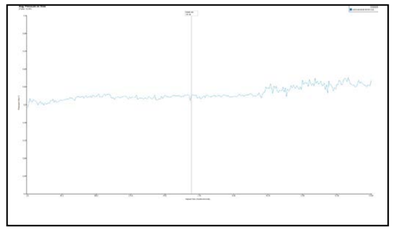

FIGURE 48: PRESSURE GRADIENT OF A SINGLE PARTICIPANT

Having extracted the data and grouped them according to their respective measurement and participant number, it becomes possible to combine the data of the tests into an overall average pressure graphic (figure 49), and an overall peak pressure graphic (figure 50).

Figure 51 & 52 explain the combined average- and peak pressure distributions spread across the surface of the bolster, respectively.

4.2.5 Conclusion & Limitations

The study findings indicate some alignment with the hypothesis regarding the spread of load. No specific area on the

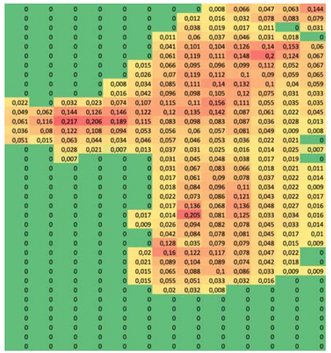

FIGURE 49: AVERAGE PRESSURE (NIJHUIS, 2024)

bolster was identified as causing peak loads for most participants. The diverse range of body shapes and sizes among participants contributed to the varied load on the bolster, emphasizing the relevance of an adjustable system over a system relying on a single inflatable air cell.

However, certain limitations need consideration. Notably, the inability to adjust the L460 seat resulted in an angle between the backrest and seat pan of around 95°. Additionally, the forward

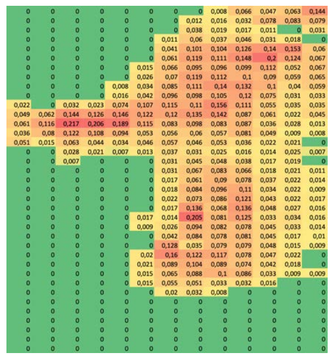

FIGURE 50: PEAK PRESSURE(NIJHUIS, 2024)

tilt of the headrest was perceived as uncomfortable by many participants. It is suspected that these factors substantially influenced the comfort ratings given by participants.

From the combined readouts absolute values per square centimeter of the contact patch can be gathered, as shown in figure 49 and 50. Although the seat was placed at a 12° angle, hereby increasing the pressure on the contact patch, the trueness of these readings, especially the peak readings, can be

questioned as the test was done at minimal pressure of the air cell withing the bolster. A more realistic setting might involve allowing participants adjust the inflatable bolster to better accommodate for their body size and preference.

It can be concluded that these pressure readings should be used as a means to localize the spread of stress on the surface instead of relying on the absolute values.

4.2.6 Design Recommendation

Examining the design objective of “Designing an active bolster adjustability system that mitigates discomfort by avoiding peak pressures on the contact patch, while maintaining simplicity in its mechanical design”, it becomes clear that there are two crucial factors in the ergonomic considerations for a new bolster: the contact patch and the adjustability feature.
In the study of Van Der Voort (2018) extensive research into the design of comfortable side bolsters is presented. From the design recommendations outlined in the study it can be concluded that for conventional bolster systems there will be a tradeoff between design that offers static comforts and those that offers dynamic comfort and support. In short, achieving dynamic comfort demands increased pressure on the contact patch to provide lateral support, whereas static comfort requires less pressure.

These findings support the conclusion made in 3.1.5, that more adjustability in the bolster area could mitigate discomfort in both static and dynamic scenarios. The study by van der Voort suggests that Height, Hardness (in kPa) and Contour (Convex or concave cut-through profile) are the largest contributors to comfort and discomfort in bolster design.

Specifically it is claimed that low (for this project defined as y-position 0, or total deflation), soft (6kPa) and convex bolsters are best for static comfort. In this case the “soft” structure refers to the suspension foam layering between the inflatable bolster and the outer layer of leather, as showcased in figure 53. Interestingly, extra convex bolsters are rated best for dynamic support, but also have declined performance in terms of discomfort.

Utilizing this information in combination with the insights acquired from the pressure mat testing, three key recommendations can be proposed for the conceptualization of the product.

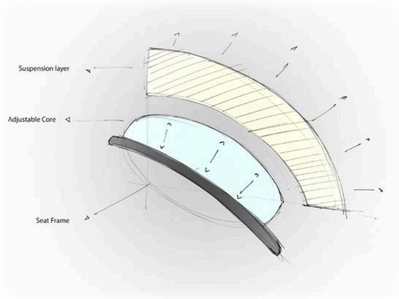

FIGURE 52: CUT-THROUGH VIEW OF MATERIAL LAYERING



System Shape and Contour

Given that the philosophy of the L460 Range Rover leans more towards the “comfort” side of the spectrum rather than being “sporty,” a suggested approach for further design considerations would be to utilize parameters aligning with a static/low dynamic design as a baseline (Duff, 2022)

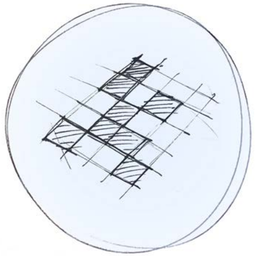

Pressure Overlay

Use the average pressure and peak pressure overlay as a foundation to pinpoint and analyze the distribution of stresses across the surface of the bolster.

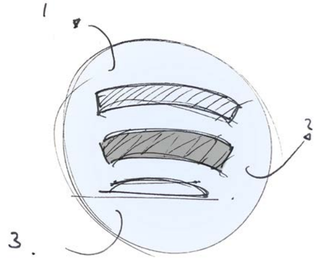

Passive Padding Materials

Explore the availability of diverse padding materials with adjustable properties is recommended to serve as a damping layer between the mechanical structure of the bolster and the outer fabric.

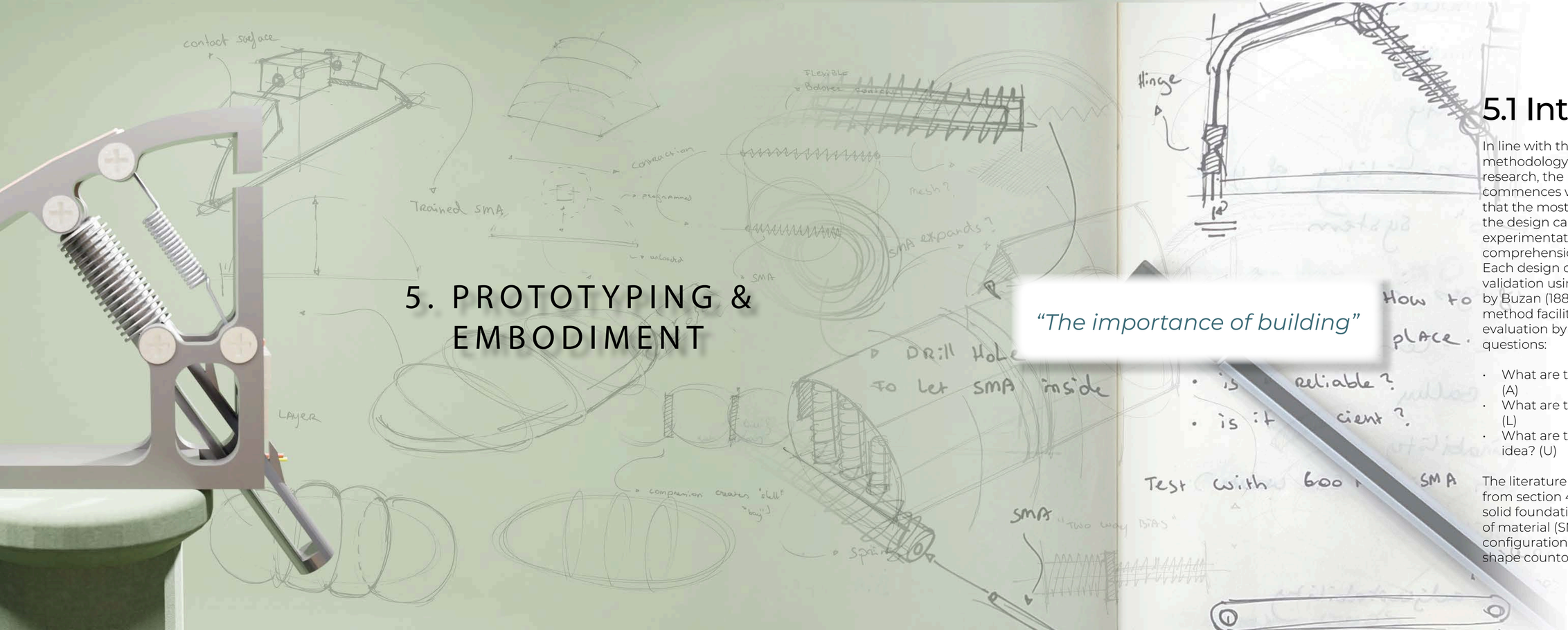

5. PROTOTYPING & EMBODIMENT

"The importance of building"

5.1 Introduction

In line with the material-driven methodology employed in this project's research, the prototyping phase commences with the understanding that the most significant value for the design can be achieved through experimentation and thorough comprehension of the actuation material. Each design decision will undergo validation using the vALUe method by Buzan (1886), when relevant. This method facilitates quick and systematic evaluation by addressing the following questions:

- What are the advantages of the idea? (A)
- What are the limitations of the idea? (L)
- What are the unique elements of the idea? (U)

The literature review and the findings from section 4 have established a solid foundation regarding the choice of material (SMA) and the desired configuration of the system (convex shape countour and pressure overlay).

5.2 Timeline

5.1.1 Ideation

Throughout the literature review and various stages of the conceptualization phase, continuous ideation was conducted by sketching potential Shape Memory Alloy (SMA) applications relevant to the bolster system. Figure 53 presents a summary of this ongoing process, showcasing the initial ideas considered most viable. These sketches are crafted and assessed based on the insights gathered in the project's initial stages, providing a foundation on which the material driven development of a prototype could take place.

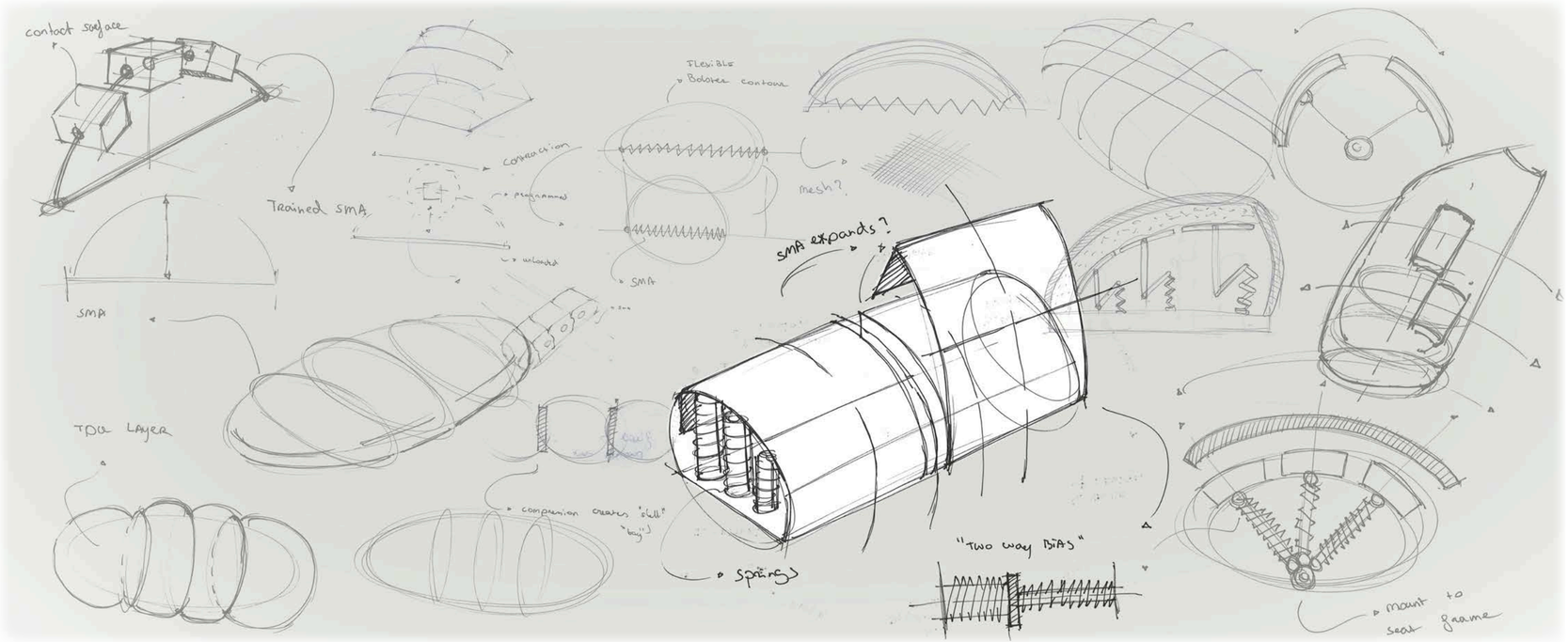

FIGURE 53: CONCEPT IDEATION SKETCHES

The drawing highlighted in white in Figure 53 was selected as an initial representation of what could provide a suitable foundation for further iteration during the prototyping phase.

This design suggestion offers the primary advantage of adhering to the outer shape of the bolster, thereby utilizing its ergonomically shaped contour as a guiding constraint for developing the kinetic system. While this approach resembles the current system and therefore lacks in uniqueness in itself, it does enable the designer to work within clear shape limitations, thus reducing the risk of overly complex initial design and aligning with the design goal of simplicity.

Moreover, adopting the philosophy of employing two or more individual moving components presents an interesting field for exploration. This approach potentially allows for individual pressure adjustments on the contact patch of the surface by enabling the system to modulate each module separately.

5.1.2 CAD Model Analysis

Utilizing the CAD file of the L460 provides an opportunity to examine the internal workings and components of the seat. Figure 54 shows the CAD model provided by JLR.

Zooming in on the Bolster section (figure 55) gives insight into the space and currently occupied by the system, which will also accommodate the new system.

It is important to note that the CAD model shows the configuration in completely uninflated position. This means 0mm of travel on the bolster.

The blue section (figure 55) of the frame shows where the air cell is currently mounted. This, combined with the foam's shape, serves as the initial reference for the model's contour.

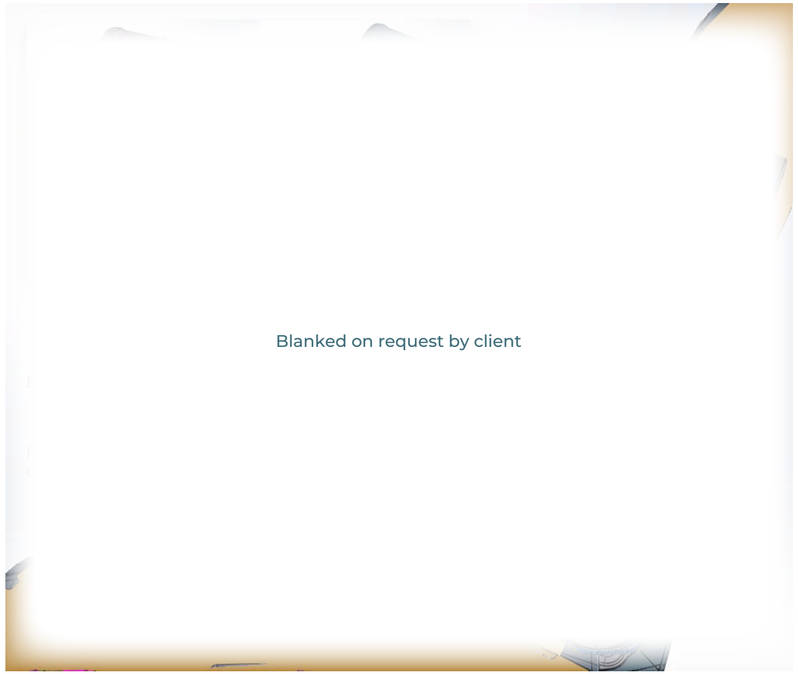

FIGURE 55: INTERNAL VIEW OF BOLSTER SECTION (JLR, 2023)

FIGURE 56: BASE PLATE OF THE BOLSTER AIR CELL (JLR, 2023)

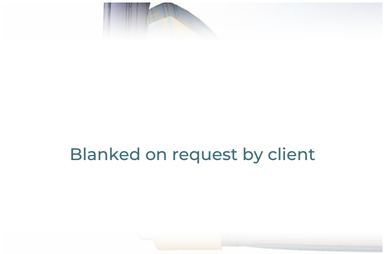

FIGURE 57: CUT-THROUGH OF BOLSTER SECTION (JLR, 2023)

FIGURE 58: CUT-THROUGH OF BOLSTER SECTION (JLR, 2023)

By employing a cut through of the seat at the dotted line in figure 55 (figure 57 & 58), similar to that depicted in Figure 10 of section 2.2.4, it becomes possible to see which components interact with the air cell of the current system and which portion of space is occupied by the foam.

Surface modeling is utilized to bridge the gap between the foam and the blue support part, revealing the potential structure's shape. Additionally, overlaying the data from the ergonomics pressure test in section 3 onto the current air cell area helps identify the active working area of the system (Figure 59).

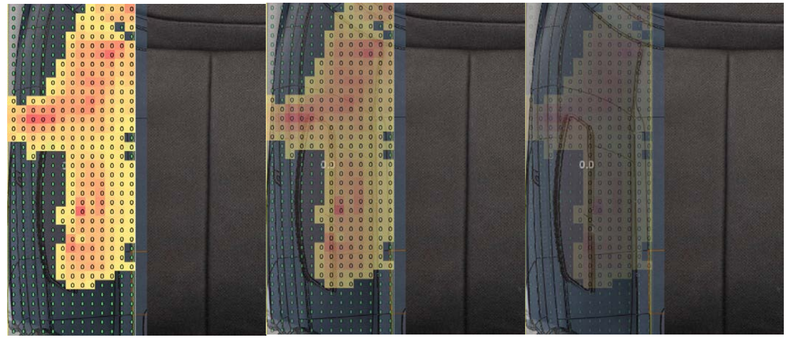

FIGURE 59: OVERLAY FROM PRESSURE MAT TESTING

By modeling the combination of the blue supports, the identified active region, and the convex contour shape of the bolster, a distinct shape emerges (figure 60).

After some applying the concept from the ideation sketching in 5.1.1, the concept of dividing the area into multiple adjustable sections arises (figure 61).

This involves segmenting the shape into slices of 20mm thickness and utilizing a single cutout to establish a base shape, shown in figure 62 & 63.

A short assesment of this idea follows:

Advantage
The concept follows the contour of the current bolster system, therefor making use of the efforts JLR has put into the performance of their bolsters.

Limitation
The concept limits exploration of shape design to enhance performance.

Unique
The concept offers increased adjustability control over the current system.

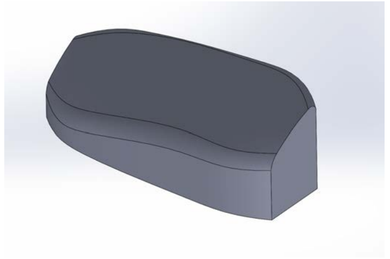

FIGURE 60: CONTOUR SURFACE MODEL

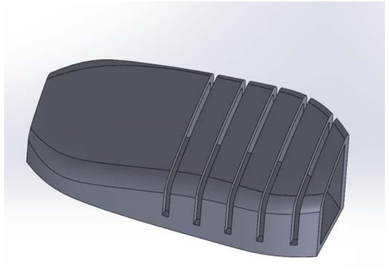

FIGURE 62: MODEL DIVIDED IN SECTIONS

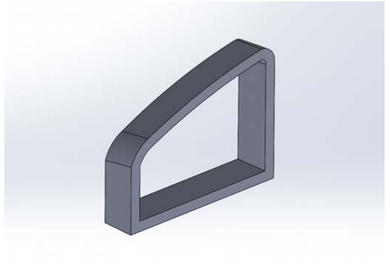

FIGURE 62: A SINGLE ROCKER



FIGURE 63: DRAWING OF A SINGLE ROCKER

5.1.3 Model Iterations

Version 1.0

A base module is designed and 3D printed (. One of the challenges encountered was creating a hinge system with minimal resistance. This was particularly crucial during prototyping, as 3D printed PLA parts tend to increase mechanical resistance in hinge systems because of the irregular surfacing.

To address this challenge, a multi-material extruder 3D printer was utilized to experiment with two TPU-based hinge systems. These systems were positioned at the front of the structure to facilitate forward rocking movement.

3D printing software CURA was used to create an interlocking structure was made to combine the PLA hinges with the PLA structure.

VERSION 1.0

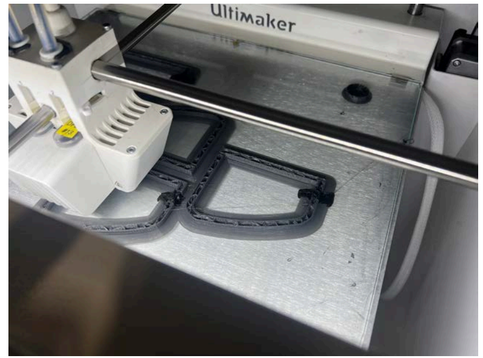

FIGURE 64: 3D PRINTING VERSION 1.0

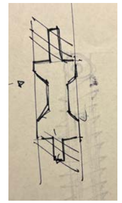

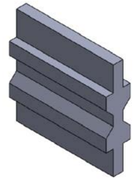

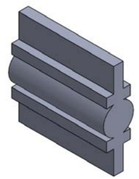

FIGURE 65: HINGE DESIGN

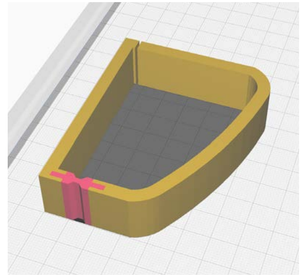

FIGURE 66: VERSION 1.0 IN CURA

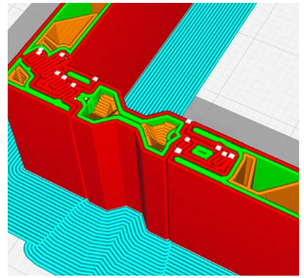

FIGURE 67: INTERLOCKING HINGE STRUCTURE IN CURA

The first three printed modules, shown in figure 68, were placed alongside a fully deflated and inflated side bolster air cell (figure 69). This comparison indicated that the shaping was already quite close to the contour shape.

The concept of a “rocker” (or tilter) system takes further shape, using SMA wire and a bias spring to actuate the top section of this model within the desired translation range of 60mm to adjust the bolster shape (figure 70).



FIGURE 68: FIRST MODULES

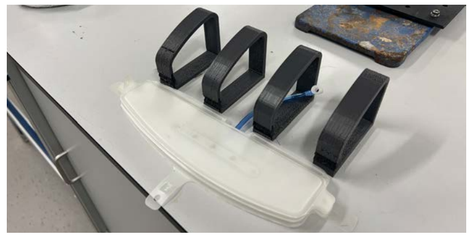

FIGURE 69: MODULES NEXT TO L460 AIR CELL

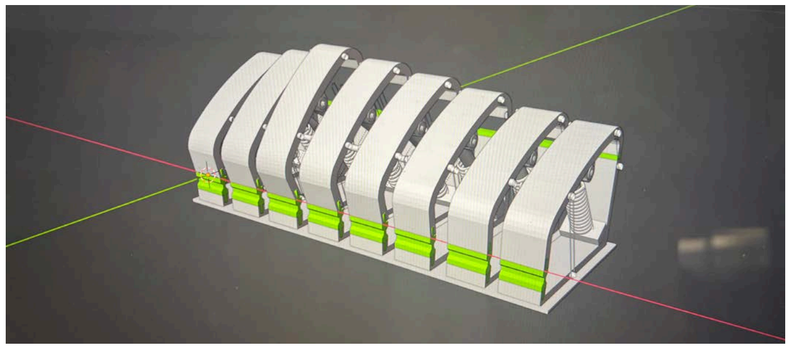

FIGURE 70: MODULES IN A ROW, SHOWING THE ADJUSTABILITY OF THE SYSTEM

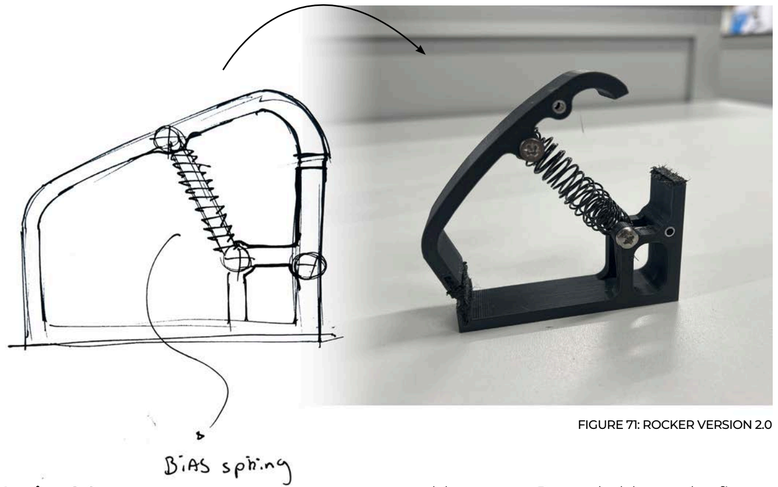

FIGURE 71: ROCKER VERSION 2.0

Version 2.0

A new version was developed to accommodate the attachment of a bias spring system and the connection of a 0.381mm diameter SMA spring to enable initial tests to ascertain if the system would actuate. Remarkably, on the first attempt with the spring, it contracted right away, as shown in figure 72 and 73.

The spring, however, did buckle when contracted (figure 73), indicating a need for improved mounting.

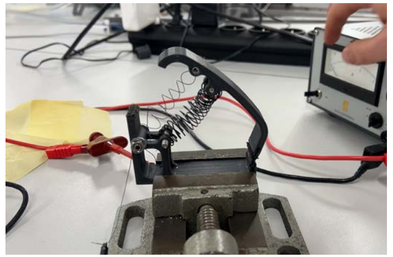

FIGURE 72: UNCONTRACTED STATE

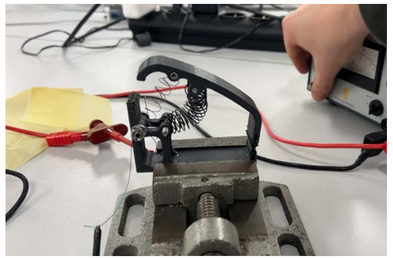

FIGURE 73: CONTRACTED STATE

Version 3.0

For the third version of the system a new mounting system was created to prevent the spring from bucking (figure 74 & 75).

During testing, it was observed that the spring contraction functioned much more effectively than before, with a noticeable decrease in perceived resistance.

Aluminum inserts were placed to prevent PLA from getting in direct contact with the SMA an melting (figure 76 & 77). In addition, threaded inserts with drilled holes were added to improve mouning of the SMA (figure 78 & 79)

Drilling holes in the threaded bolts on the side of the structure in combination with aluminum inserts at the top proved to improve the strength and easy of mounting significantly.

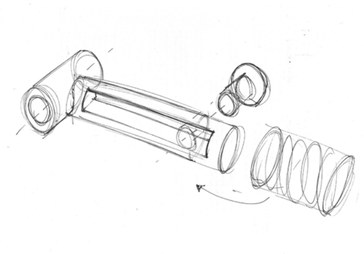

FIGURE 74: IMPROVED MOUNTING



FIGURE 75: VERSION 3.0



FIGURE 76: ALUMINIUM INSERTS

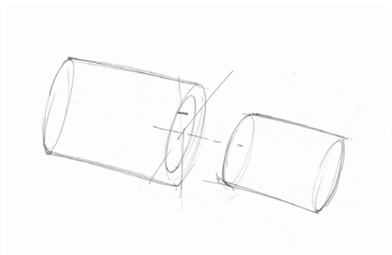

FIGURE 77: INSERTS DRAWING

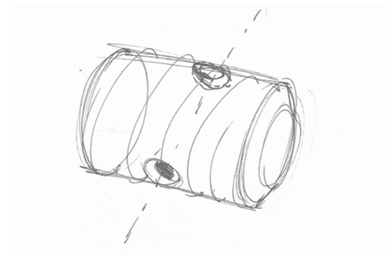

FIGURE 78: DRILLED THREATED INSERT

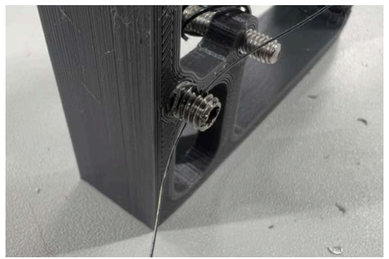

FIGURE 79: WIRE MOUNTING WITH INSERT

Version 4.0

With the improved mounting, the data collection on the forces exerted by the spring became possible. Additionaly, an examination of the range of movement would take place.

The measurements of the passive spring used in the initial prototypes were unknown. As a result, a new spring with known properties was introduced (figure 80).

Unfortunately, this new spring proved to be quite stiff for the system, making it challenging to achieve full contraction, even with two .381 SMA coils or a 1mm diameter SMA spring.

A main takeaway from this seems that more research is needed into the effect of SMA and bias coil/wire parameters to enable the desired contraction.



FIGURE 80: PROPERTIES OF THE NEW SPRING

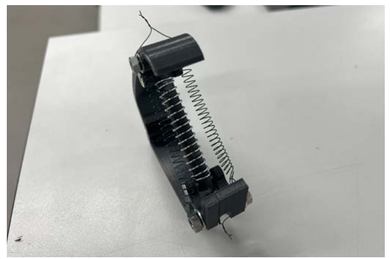

FIGURE 81: DOUBLE .381MM WIRE MOUNTING

The force exerted by the bias spring at full compression shows 27.1N (Figure 82. This is more than the 22N of heated pulling force the .381mm SMA wire is rated for according to Dynalloy (2023) (Table 5).

Both the dual .381mm spring (figure 83) of the single 1mm spring were unable to contract this bias spring more than a few mm.

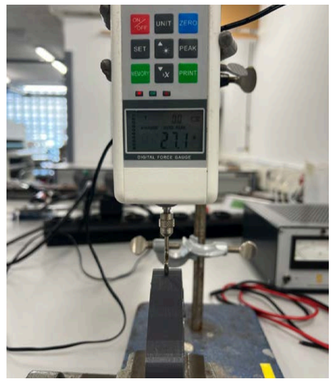

FIGURE 82: FORCE APPLICATION OF THE NEW SPRING

Diameter (mm)	Resistance ($\frac{\Omega}{m}$)	Heating pull force (N)	Current estimate for 1s (mA)	Cooling pull force (N)
0.025	1425	0.09	45	0.04
0.038	890	0.2	55	0.08
0.05	500	0.35	85	0.14
0.076	232	0.78	150	0.31
0.1	126	1.4	200	0.56
0.13	75	2.186	320	0.87
0.15	55	3.14	410	1.26
0.2	29	5.58	660	2.24
0.25	18.5	8.73	1050	3.49
0.31	12.2	12.55	1500	5.02
0.38	8.3	22	2250	8.83
0.51	4.3	34.91	4000	13.96

TABLE 5: SMA HEATED PULLING FORCES (DYNALLOY, 2023)

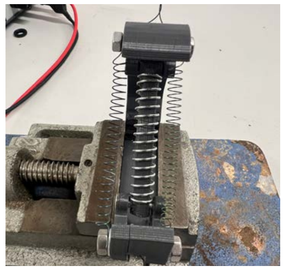

FIGURE 83: DUAL .381MM SPRING SETUP

Actions were taken to determine the correct wire parameters by using supporting literature.

According to Rao et al. (2015) there are three things to consider when designing a bias spring system (figure 84):

1. SMA Wire geometry
2. Bias spring selection
3. Actuation temperature

Firstly, wire geometry parameters such as diameter, length and number of wires are dependent on the use case that is presented. As can be seen in figure 10, of section 2.2.4, we need at least 60mm of translation on the largest section of the bolster (and no more than 10% compression at test load).

It is stated that SMA wire can recover between 6 to 8% strain under ideal condition, but due to potential fatigue constrains the system will be limited to 5% strain.

Current prototype only allows for 30mm of travel (Figure 84). constant is.

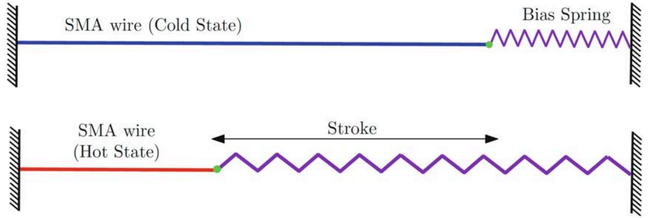

FIGURE 84: BIAS SPRING MECHANISM EXPLAINED (RAO ET AL, 2015)





FIGURE 85: COMPRESSION RANGE OF CURRENT SYSTEM

Using Hooke's law it can be determined what the spring constant of the current spring is.

With the knowledge that in tested state the spring is 50 mm in length and the force applied is 27.1N at 20 mm compression

k = - F / x

k = - 27.1 N / 0.020 m

k = 1.355 N / mm

This would mean that for 30mm compression the force would be approximately 40.65 N, higher than the rated pulling force of the wire.

As tested in 2.2.2 the outer edge of the aircell can deliver 11.2 N of force.

60mm of travel (along the red line in figure 86) and 11.2 N of force are needed for this prototype. Therefore the following spring constant is calculated:

k = - F / x

k = - 11.2 N / 0.060 m

k= 0.187 N/mm

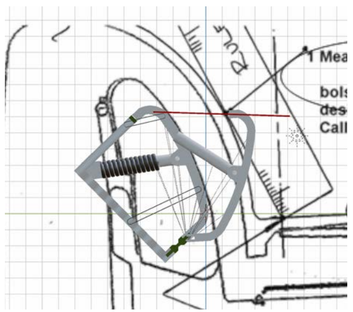

FIGURE 86: MOVEMENT RANGE OF THE PROTOTYPE

After consideration, it was determined that a spring with a deformation range of 60mm and similar overall proportions to those desired for the system was needed.

Amatec, a Dutch reseller of springs, offers the D21840 compression spring, which closely matches the calculated parameters (see figure 87) (Amatec, 2024).



- 0.80mm wire diameter
- 10.80mm outer diameter
- 96.50mm unloaded length
- 28.5mm loaded length (L1)
- 12.82N Force at L1
- 0.19N/mm spring constant

FIGURE 87: D21840 PROPERTIES (AMATEC, 2024)

The testing phase began to determine the most suitable application of wire shaping; coiling or keeping it straight.

It's important to note that this testing was not conducted with the D21840 spring, but with a much weaker spring to establish proof of the working principle before applying additional loads.

Research indicates that sufficient contraction of a constrained, untrained wire can be achieved, provided that all parts that should remain immobile are properly constrained (Liu et al., 2022).

The initial test setup involved using an unprogrammed wire with a diameter of 0.381mm, cut to a length of 600mm.

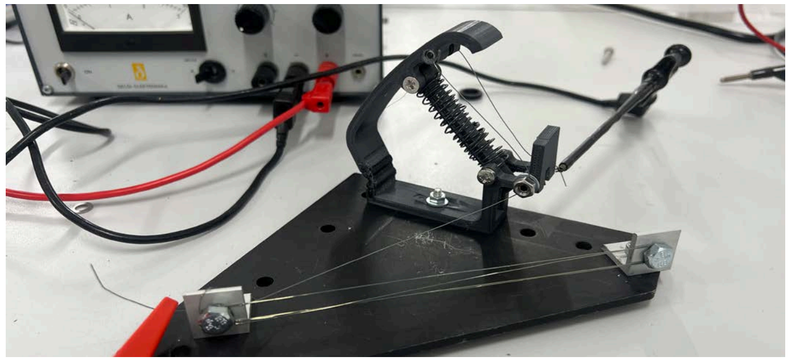

FIGURE 88: ACTUATING A STRAIGHT, CONSTRAINED WIRE



Results showed that upon actuation, the wire initially pulled but then reached a plateau, failing to achieve the full range of motion required (figure 88).

Given the complexity of achieving straight wire actuation, even with tries with other constraining methods (figure 89), When testing a well constrained wire, some contraction is shown. However, it is deemend too complex at this point to keep the constrained area under 5% deformation, whereas using a spring has given more consistant results in contraction.

The decision is made to continue with a spring based system, where more efforts are put into development of an accurate SMA spring an efficiency of the overall mechanism.

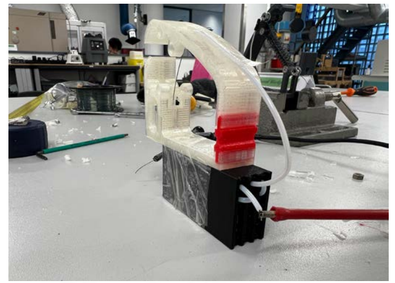

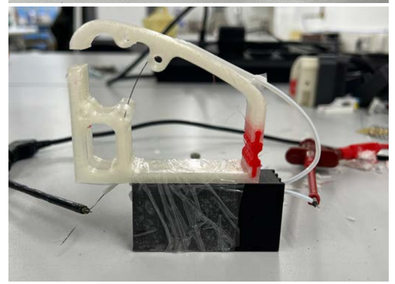

FIGURE 89: ALTERNATIVE CONSTRAINING OF THE WIRE

Version 5.0

The upper mounting of the SMA element is placed parallel to the bias spring to have as little loss of contraction force as possible. The connection for copper wires go into the structure (figure 90). A version is made with a full integrated wire fittings (figure 91).

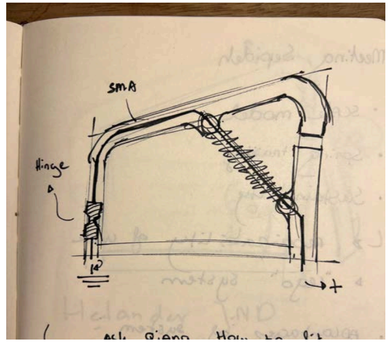

FIGURE 90: VERSION 5.0

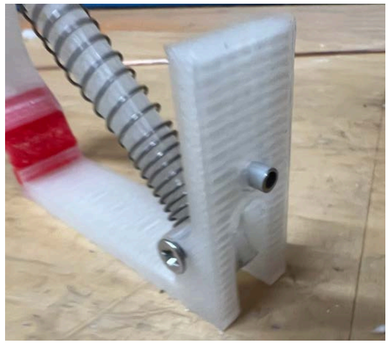

FIGURE 91: INTEGRATED INSERTS FOR WIRE MOUNTING

The new spring is utilized to accommodate 60mm of movement and is positioned lower within the structure to achieve a total spring length of nearly 100mm (refer to figures 92).

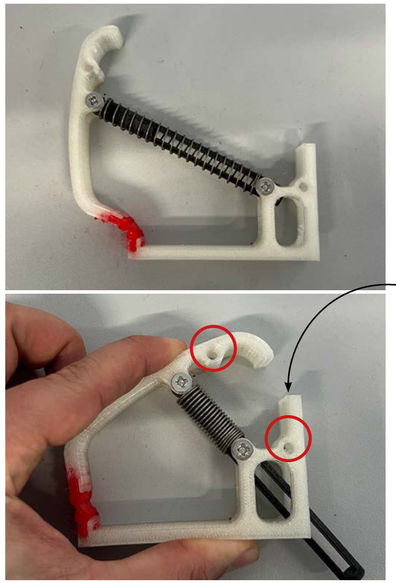

FIGURE 92: INCREASED RANGE OF MOTION

In version 4.0, conventional mounting points were used for the SMA spring. However, this approach proved problematic during testing, leading to the decision to make adjustments in the next version by removing the holes for the threaded inserts. In version 5.0, the spring will be constrained at the top and bottom of the structure itself (figure 93), and through trial and error, the ideal mounting configuration will be determined.

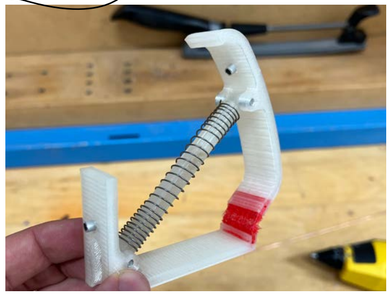

FIGURE 93: VERSION 5.0

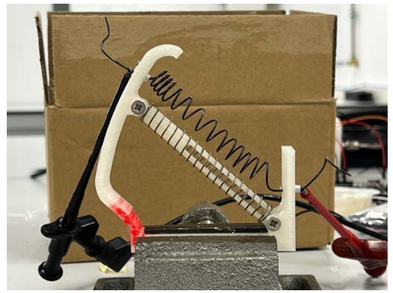

FIGURE 94: INCREASED RANGE OF MOTION

The individual components of the system were sanded, sodablasted and greased in order to reduce as much drag friction as possible. Although the movement was much smoother, the single .381mm SMA was not enough to contract. As explained by Liu et al. (2022) deviation in pulling force can get as high as 27% when nearing maximum loads, which could be an explanation for this problem.

This insight prompted another effort to theoretically determine the SMA spring parameters.

The 2D sketch in Figure 95 provides an overview of the forces acting on the system that directly affect the spring parameters. For simplicity, any energy loss due to resistance in the system is not considered.

In the sketch, springs k1 represent the (SMA) Nitinol spring and k2 the bias spring, respectively. It is known that F2 must exert 11.2N of force to provide sufficient support for the user.

The aim is to determine the exact force application of the SMA.

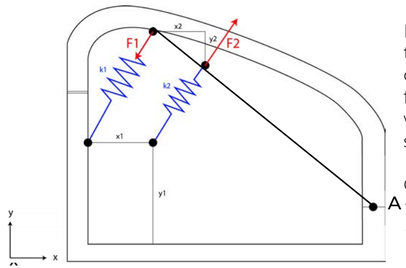

FIGURE 95: 2D SITUATION SKETCH

Since the force acting on F2 is known, the direct distance between point F1 and F2 must be known to calculate the moment of F1 around point A. For the sake of simplicity the line between A, F1 and F2 is considered straight.

Distance F1 to F2 is 15mm and distance F2 to A is 60mm.

$$Moment\ A = -F1 \times 0.075 + F1 \times 0.060.$$

$$-F1 \times 0.075 + 11.2 \times 0.060 = 0$$

$$F1 = 8.96\ N$$

Now that we know the force and are able to measure that the SMA spring must deliver around 9N of maximum pulling force, an indication can be made on what parameters are needed for the SMA spring.

One large obstacle in this, however, is that in contrast to conventional springs, deflection and load behaviour is not linear for SMA springs, as shear and spring constants change with strain.



Given the relatively high strain required from the SMA coil in this project, it's important to note that the behavior of the material can vary significantly during the activation cycle (Ishii, 2011).

While an educated guess could be made regarding how the spring might behave, it's essential to recognize that factors such as production, treatment, and shaping conditions can have a substantial effect on the material's performance, as described by Ishii (2011). Additionally, the lack of prior experience working with SMA spring physics leads to the conclusion that efforts would be better spent elsewhere.

Therefore, the decision has been made to over-engineer the spring (within reason) in order to achieve a working proof of principle for the concept. This will involve applying a much higher heated force than theoretically needed.

Version 6.0

Two additional versions are made, one with a double SMA coil configuration (0.381mm) and one with a single coil configuration (1mm)

All three coils have the same configuration of 15mm length and 10 coils spaced evenly (figure 96 & 97).

(tested) activation ranges for both material were 40 to 70 degrees Celsius (figure 98).

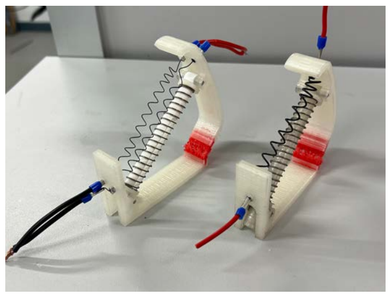

FIGURE 96: INCREASED RANGE OF MOTION



FIGURE 97: COIL WINDING BEFORE TREATMENT

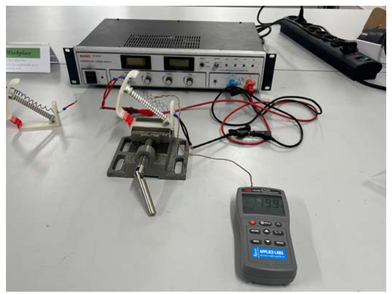

FIGURE 98: TESTING OF ACTIVATION TEMPERATURES

While testing the 1mm diameter springs showed much more effective than the 0.381mm dual setup. Although the latter could be activated below 5s at 3A, the contraction would not show the desired range of motion, whereas the 1mm springs would contract at similar speeds and reach nearly 60mm of contraction (figure 99).

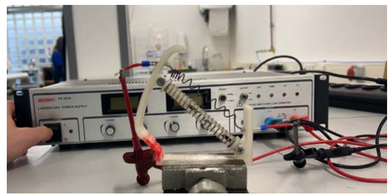

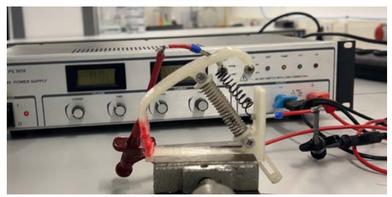

FIGURE 99: TESTING OF ACTIVATION TEMPERATURES

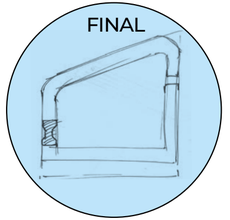

Final Version

After making the final decision on SMA coil geometry (1mm, 10 coils, 15mm), the assembly of the final prototype could begin.

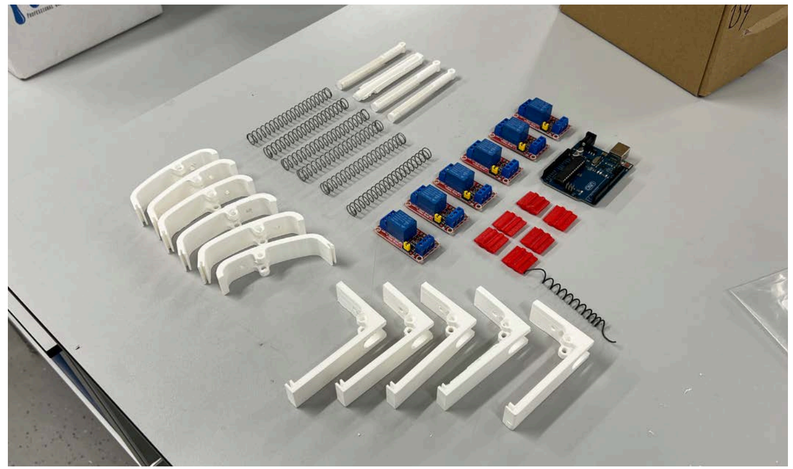

FIGURE 100: STARTING ASSEMBLY OF THE FINAL PROTOTYPE

Firstly, assembling 6 individual actuators after preparing the springs (figure 101 & 102), then lasercutting and preparing the baseplate (figure 103).

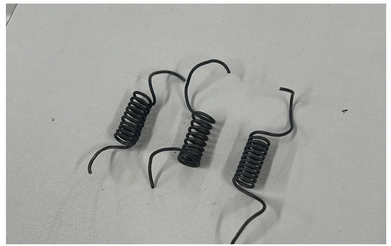

FIGURE 101: 3 OF 6 SMA SPRINGS

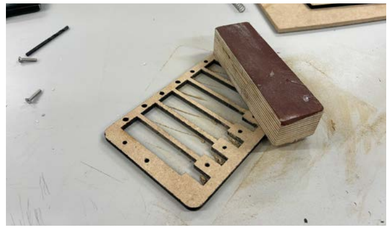

FIGURE 103: MDF BASEPLATE

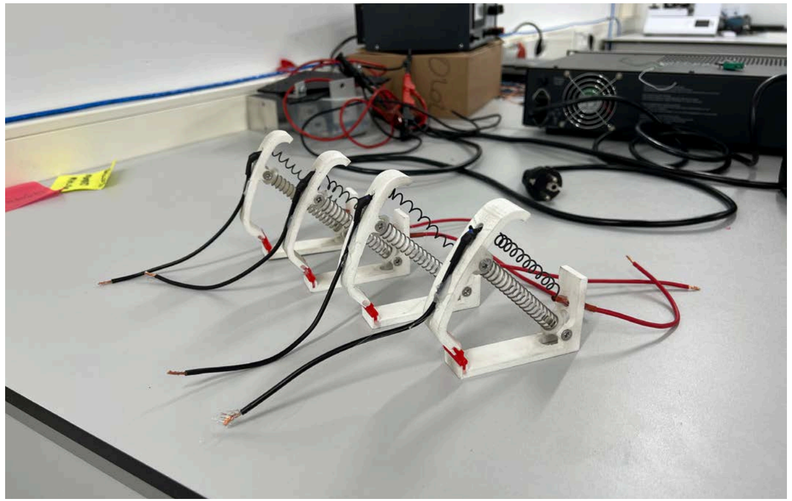

FIGURE 102: 4 OUT OF 6 ACTUATORS

Electronics

To control the device an Arduino system was created by the author to actuate the individual rockers. Explained in figure 104 is the schematic overview of the Arduino circuit. The ratchet system is not present in the physical prototype due to the added complexity. Please note that the system makes use of 6 individual 5V actuated relays to control the external power supply. These relays are places in parrallel of eachother.
The Arduino code can be found in appendix E.

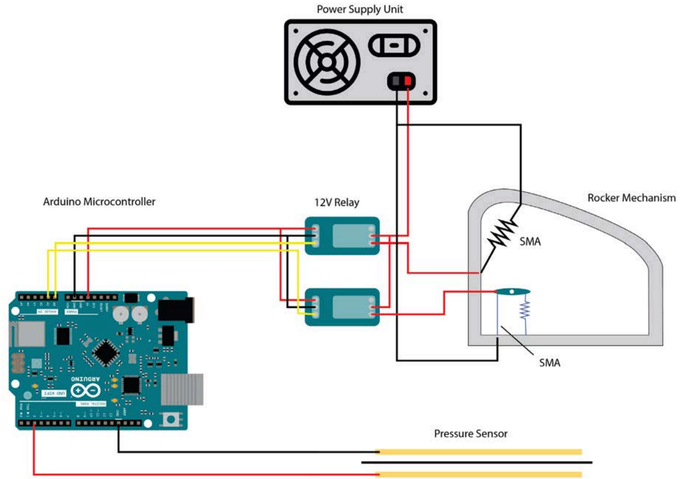

FIGURE 104: ARDUINO SCHEMATIC OVERVIEW

Pressure Sensor

To enable the bolster to actively adapt to the shape of the occupant, pressure sensors were created using a layer of Velostat material and two electrodes positioned on either side of the material, as depicted in figure 105 & 106. External pressure can be determ5ned by measuring the (increasing) resistance between the electrodes. Unfortunately, even after calibration, these actuators do not achieve the desired accuracy but effectively function as an “on/off” signal for detecting pressure on the surface of the structure (W. Song, personal communication, 2024).

In the coding for the actuator, each sensor was tested and a threshold value was set for the Arduino to receive an “on” signal (appendix E).

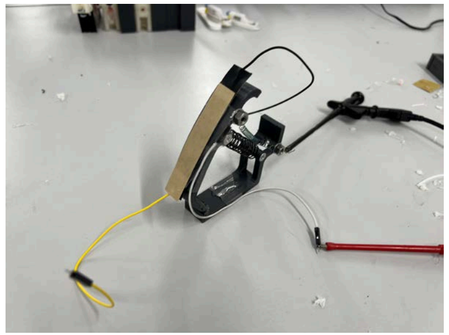

FIGURE 105: VELOSTAT PRESSURE SENSOR APPLIED

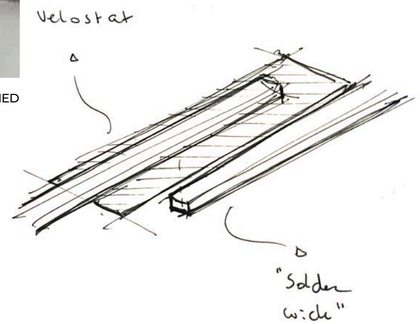

FIGURE 106: PRESSURE SENSOR SKETCH

Final Assembly

Once the individual components were assembled, the final prototype was assembled (figure 107 & 108).

Most connections in the final assembly are mechanical, utilizing nuts and bolts. However, to enhance sturdiness, hot glue was employed where necessary.

An overview of the full assembly is shown on the next page spread (figure 109).

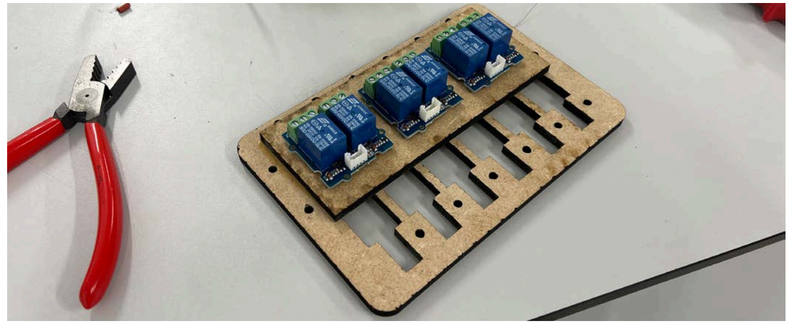

FIGURE 107: 5V RELAYS MOUNTED TO THE BASE PLATE

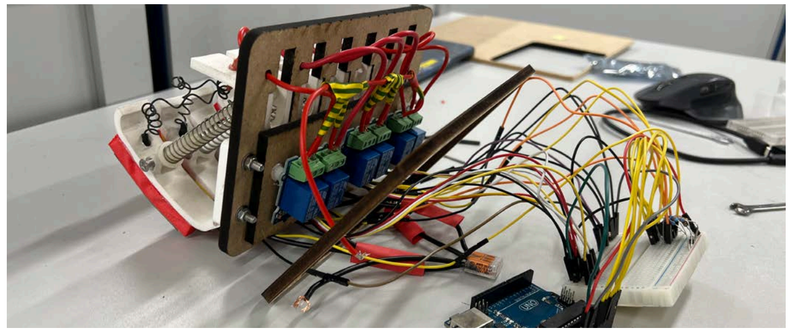

FIGURE 108: EXPOSED WIRING OF THE PROTOTYPE

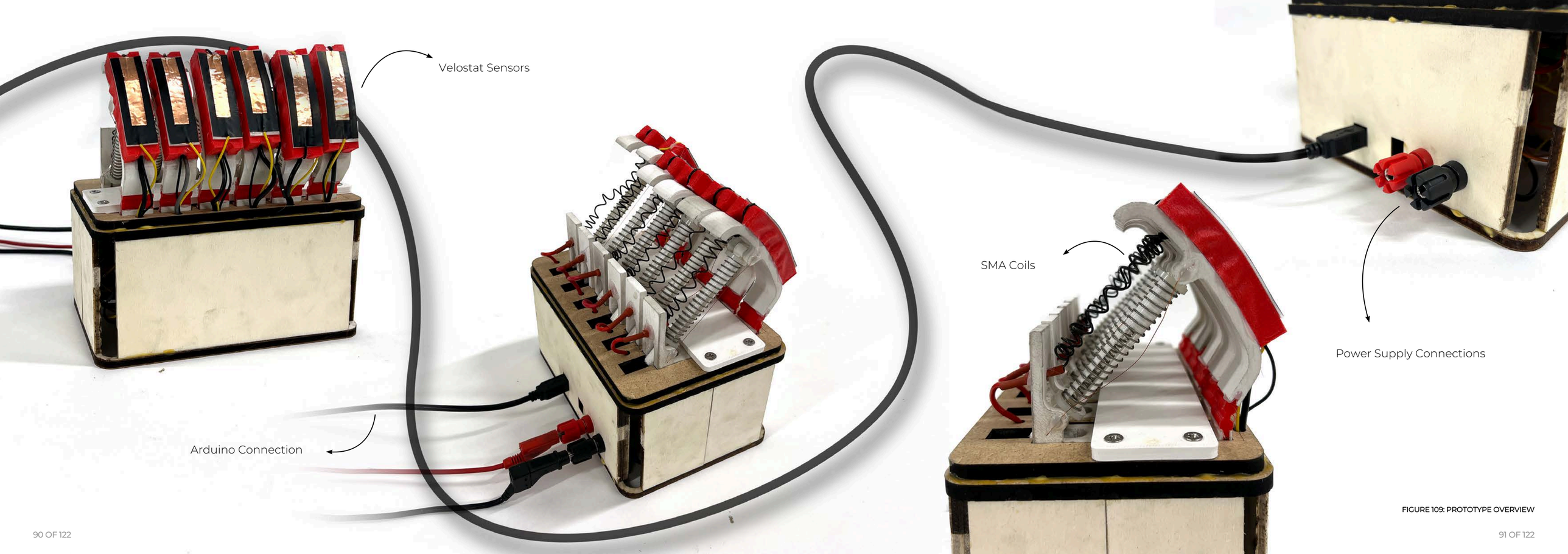

FIGURE 109: PROTOTYPE OVERVIEW

6.FINAL CONCEPT OVERVIEW



6.1 Introduction

After the extensive prototyping, this section showcases the final concept through high quality pictures and descriptions of its workings.

Shaped by the Human Contour, Driven by Nitinol

The SMA-based bolster system actively adjusts its shape to accommodate its occupant by detecting the areas of its surface in contact with the human body.

Through sensing the force and duration of loads on the contact patch, the system dynamically adjusts to alleviate overall discomfort and prevent sustained periods of peak pressure, all contributing to creating as much comfort as possible for the occupant.

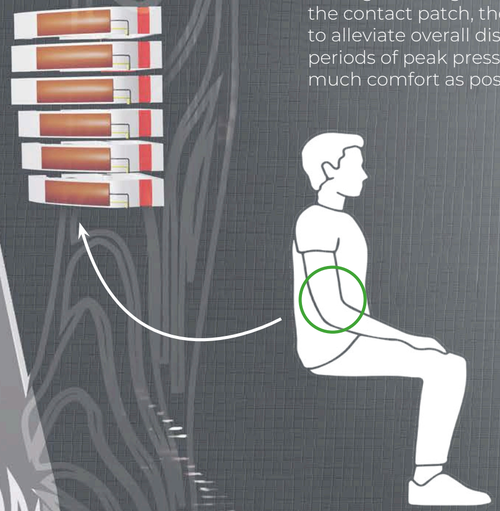



New System, Same Location

The SMA-based system is positioned in the same location as the conventional pneumatic-driven bolster system, following the existing contours of the L460 seat bolsters. This ensures that the proven shaping of the seat still functions as intended.

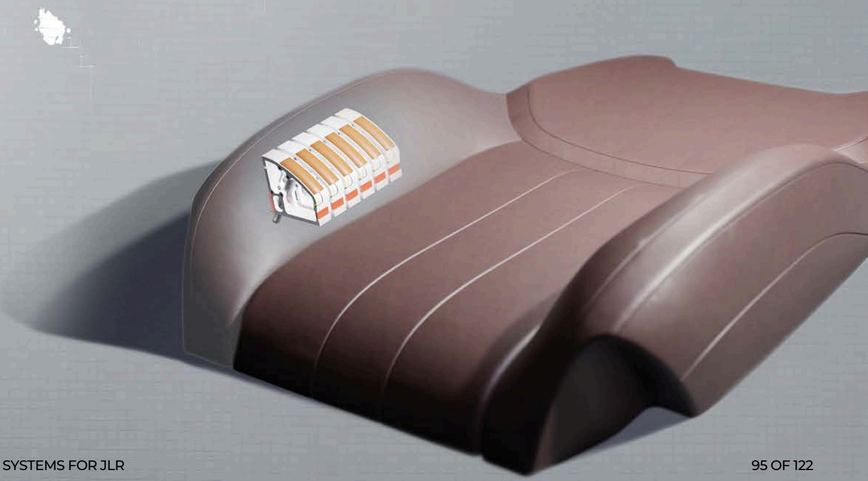

Efficiency and Simplicity

Efficiency and simplicity are key aspects of the proposed concept. With 6 individual actuators, maintenance becomes straightforward as they are easily interchangeable. The design emphasizes the use of SMA as the main kinetic element, keeping the number of individual components to a minimum without compromising performance.





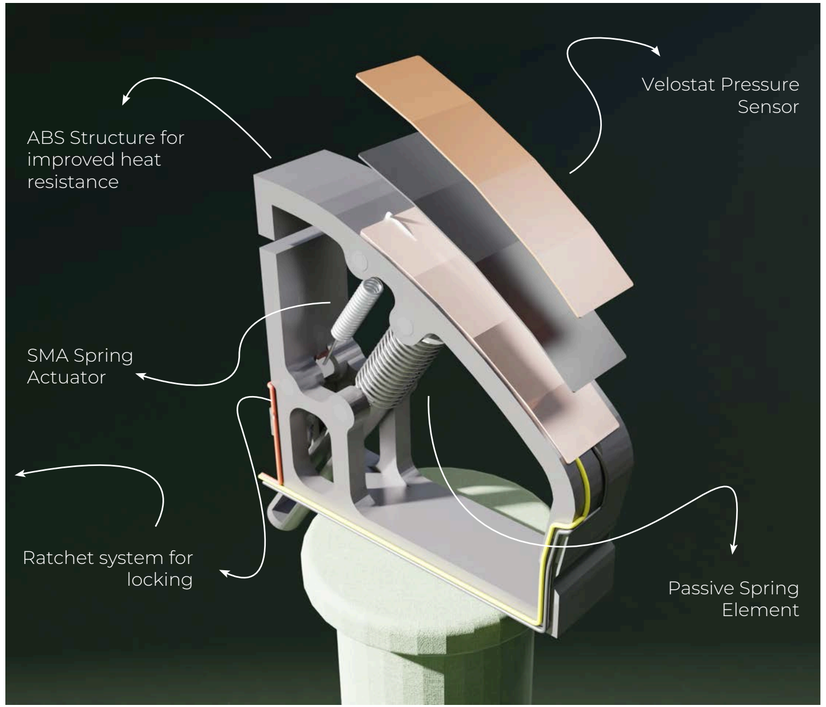

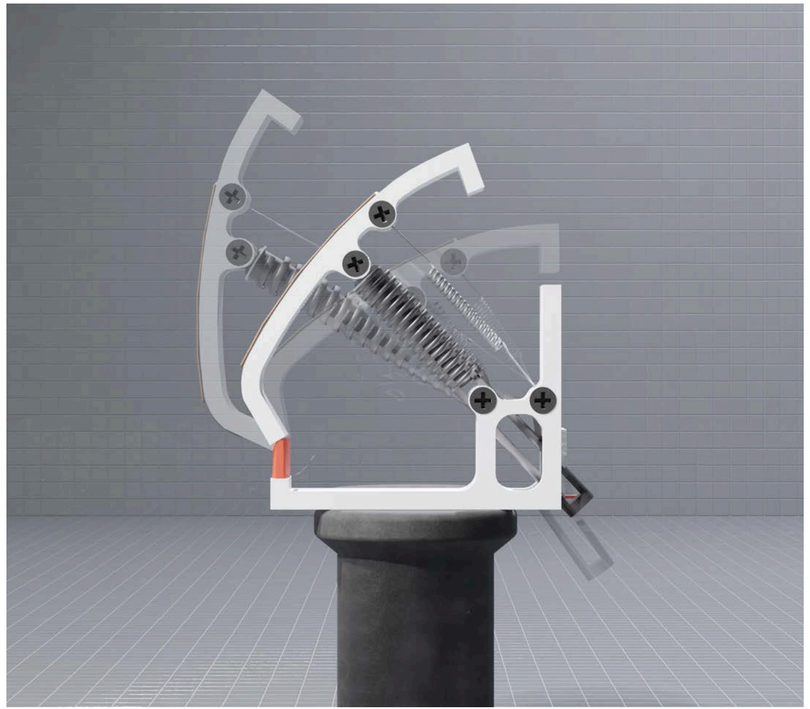

Comfort for Everyone

The actuator operates in 3 distinctive steps of motion, described as “just noticeable increments,” ensuring efficiency in comfort by adjusting within ranges perceptible to humans.

Moreover, by providing adjustability control over smaller sections of the bolster rather than one large area, unlike the current system, comfort can be ensured for a broader range of body shapes and sizes.

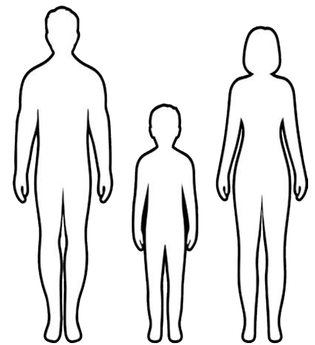

Sustainable and Effective

Simplicity in design was a crucial focus during the development of this system. At every stage, considerations were made regarding durability, actuation performance, and simplicity to create a product that performs effectively while minimizing energy impact. Utilizing SMA as the main component allows for retraining when its capability diminishes, ensuring that individual springs can be repurposed without sacrificing performance.

The easy access flayout of the design facilitates quick repair of individual modules and swift disassembly of parts for potential recycling, further enhancing sustainability and minimizing environmental impact.

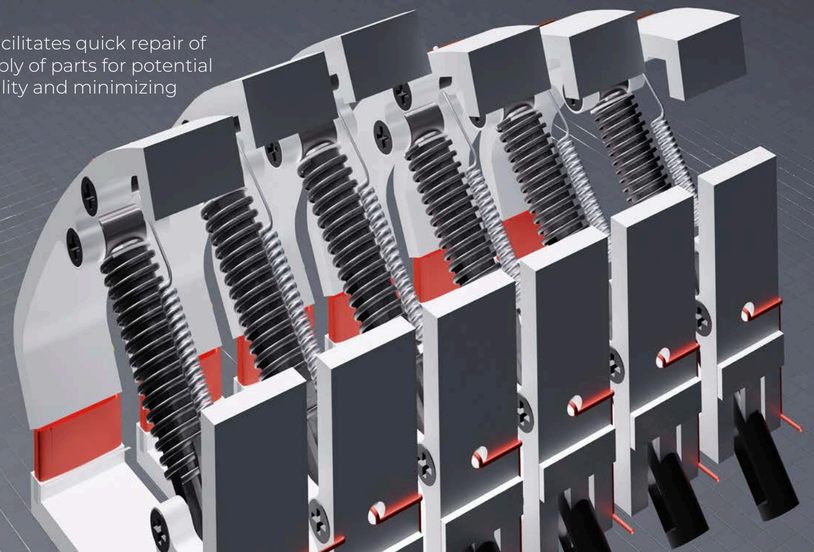

References

Ishii, T. (2011). Design of shape memory alloy (SMA) coil springs for actuator applications. In Elsevier eBooks (pp. 63–76). https://doi.org/10.1533/9780857092625.1.63

Liu, Q., Ghodrat, S., & Jansen, K. (2022). Modelling and mechanical design of a flexible tube-guided SMA actuator. Materials & Design, 216, 110571. https://doi.org/10.1016/j.matdes.2022.110571

Rao, A., Srinivasa, A. R., & Reddy, J. N. (2015). Design of Shape Memory Alloy (SMA) actuators. Springer.

7.EVALUATION

7.1 Validation

In order to have a proof of concept, the prototype must be put to the test. This is done to investigate if the proposed concept in embodied state can show the intended movement and response to input. It is evaluated how the prototype compares to the current system, while bearing in mind their current technology readiness level (TRL).

Does the proposed prototype give a viable proof of concept?

Movement and Load bearing:

When attaching the prototype to a power source and running the code on the Arduino circuitboard, the system can be tested.

Firstly, when the pressure sensors are pressed on one of the actuators, the code says that the the two adjecent modules must activate. In testing it was shown that this is in fact the case. The actuators consistantly contract and expand as intended (figure 109).

Additionally, the 1mm diamter SMA springs used seemed to have no problem contracting the 11.2N force springs.

Actuation time and consistency:

Activation time for the pneumatic JLR system was 8.8s in an unloaded scenario. For the new system measured actuation times in contraction were averaged around 5s, however in textension the times could get as high as 20s. This is due to the SMA having to cool down to reduce in stiffness.

Regarding consistency, the SMA springs failed to show consistent travel when



FIGURE 109: COMPRESSION OF THE SYSTEM

retracting. The activation and response of both the springs and the sensors would consitently work, however not all springs would contract the similar amount every time.

Power consumption:

For a single activiation cycle of the pneumatic JLR system the following power consumption was measured:

$$Power(P) = Voltage(V) \times Current(I)$$

$$P = 12.6V \times 0.02A$$

$$P = 0.525\ W$$

The prototype showed the 5.4A and 2.5V for a single retraction of **one** actuator , which gives:

$$P = 2.5V \times 5.5A$$

$$P = 13.75\ W$$

Weight:

Both devices were weighted to investigate how they compare to each other.

The pneumatic pump and bolster air cell together weighed 412 grams (see figure 110)



FIGURE 110: WEIGHING OF THE PNEUMATIC SYSTEM



FIGURE 110: WEIGHING OF THE PNEUMATIC SYSTEM

The SMA-based system, including the enclosure, weighed 798 grams. Without the enclosure, the system weighed 445 grams.

7.2 Conclusion

The main questions to answer are:

- *Does the proposed prototype give a viable proof of concept?*
- *Does the final design align with the design goal?*

Firstly, looking at the validation results, it can not objectively be determined if one system functions better than the other as they both operate at different levels of “technology readiness”.

The pneumatic system operates at TRL level 9, meaning the system has been proven in an operational environement. In other words, it is a finished product.

The proposed SMA based bolster system seems to be in the neighbourhood of TRL level 4, meaning that there is some sort of experimental proof of concept, but concept has not been yet been completely validated in a professional testing environment.

Given this situation, it is interesting to assess the potential the SMA based system shows by exploring the sections which the pneumatic outperformed it.

The system, as described in the prototyping section, and especially the spring is in theory overengineered. This means that the thickness of the springs is much larger than needed in an ideal situation.

The result of this is that contraction and expansion performance is affected in the form of increased power consumption and longer cooling times due to the increased specific heat capacity.

The fact that, while eventhough this is the case, the system could deliver performance close to what was specified in the list of requirements, shows the potential of the system.

Not only is it clear that much can be won in reducing system friction and optimizing spring geomeometry, the concept shows that performance similar to that of the conventional system could be achieved without having an overly complex device.

Both in terms of weight and performance the system shows an SMA based adjustment system could be suitable for application in car seats.

Furthermore, during the project the following design goal was formulated:

“Designing an active bolster adjustability system that mitigates discomfort by avoiding peak pressures on the contact patch, while maintaining simplicity in its mechanical design”

After finishing the validation of the system and seeing that it is possible to achieve seperate adjustability across the surface area of the bolster, the design goal can be considered as achieved.

With that it must be noted that the research presented in this thesis no yet sufficiently shows how discomfort would be mitigated by the system. The system shows how that seperate adjustability can be achieved, further research could show what the ideal configuration for this would be.

To conclude, this thesis shows that improvement in performance and design of (active) bolster systems could be achieved by using shape memory materials

7.3 Recommendation

Recommendation

In the span of the 20 weeks that have been spent working on this prototype, it has come a long way in providing a proof of concept but is still far from a finished product. The aim of this project has been to explore the implementation of shape memory materials Jaguar Land Rover seats to benefit their adjustment capabilities. Although an initial step has been made towards showing what could be possible when rethinking the way kinetic systems are designed, to really have a usable product a range of subjects demand a deep dive for further exploration.

SMA spring geometry and treatment

As explained in this report, the design of SMA springs poses significant challenges as nitinol shows nonlinear contraction behavior when under load. Nitinol has proven to be a very efficient source for creating kinetic actuation. However, getting an SMA spring to contract as intended is not only subject to choosing the correct parameters for the physical shape of the spring but is greatly determined by every step in its composition, shaping and treatment of the material. It seems that having a standardized process for the creation of these springs as well as how they are mounted to the heating source is a first step into getting repeatable results from springs. When further exploring the embodiment of an SMA based bolster system, keeping the variation in variables that could influence the performance of the material to a minimum seems crucial. In addition, efforts into extensive modelling and testing of these springs could show beneficial in increasing their efficiency, extracting as much performance from the energy put in as possible. Further efforts should rely on standardized (i.e. not homemade) springs as much as possible to really be able to benchmark their performance and systems designed around them.

Spring number and placement Break even value

From the testing conducted in this research as well as when looking at contemporary SMA application, it could be assumed that SMA thrives when applied at very small scales. As can be gathered from the documentation in this report, load and actuation time deviations rise as the size of the material used increases. What has not been investigated thoroughly in this report, but might show very valuable, is the creation of an actuation system with a multitude of smaller diameter springs connected in series, instead of a single larger diameter SMA spring. By doing this it could be that fast actuation times as well as low current demand could be achieved, in comparison to the system proposed in this system which demand relies on relatively high current. In designing such a system, the investigation of a breakeven value or approach could be proposed. Having a break-even value for where a multitude of small springs outperforms a single large one and vice-versa could again lead to extracting as much efficiency from the material as possible.

Repariability

Further research into easy access of the modules and their components could show beneficial for enabling easy repairability, and therefore increased sustainability of the system.

Passive distribution layer

This subject has been touched on multiple times in the report, but was deemed to large of a subject to investigate, is the application of a passive suspension layer on top of the system.

Modern 3D printing solution allow for the creation of a suspension layer that can have variable stiffness according to how the layering of the material is designed.

Exploring the application of this as an alternative to foam in combination with the system proposed in this thesis could be an interesting combination of pressure distribution methods. The passive element of the 3D printed structure could be tuned according to the workings and limitations of the SMA system, hereby “filling” in any gaps in capability that might be there.

Appendices

Appendix A: Testing Procedure

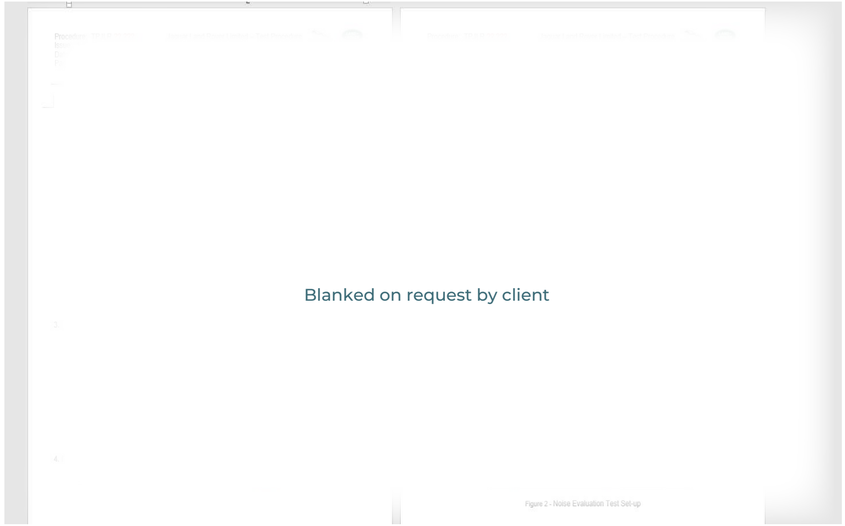

Appendix B: HASEL Production

Hasel Test



Ordered and received materials:

Silicone oil 50cst (same viscosity as FR3 Cahill used in other tests)

BOPP Foil 20 micron (smallest size available)

Bare Conductive Electric Paint

Copper conductive tape



Procedure

Extensive research can be found describing procedure and techniques in fabricating HASEL actuators. A paper by Mitchell et al. (2019) describes one of the most common techniques in assembling an actuator.

Appendix B: HASEL Production

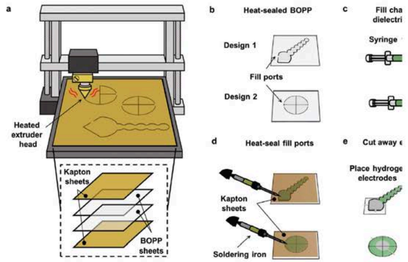

The procedure seems to be the same for most literature available:

1. Using heat to cut and seal the BOPP sheet into the desired shape and pocket.
2. Leaving a 2mm fill port to inject the liquid dielectric into.
3. Injecting the fluid.
4. Using a soldering iron to seal fillport.
5. Cut away excess BOPP.
6. Apply electrodes.

This procedure seems the most tested and straightforward method to produce the actuators, however another paper by P. Wissman et al. (2020) describes the use of a laser cutter to cut and heat seal the BOPP, instead of a heat extruder or pre-formeod heating plate.

Since there are several laser cutters available at the IDE faculty and no heat extruders, this seems a more viable way to produce first prototypes. Wissman et al. concludes that by using a laser cutter design space and convenience are enhanced.

Steps:

1. Clean + side with isopropyl alcohol
2. Rub together to induce static

Table 1: Laser engraver parameters used on PLS6MW (ULS).

Operation	Power (%)	Speed (%)
Cut	1	10
Cut and Seal	50	100

3.

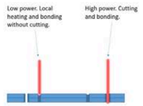

Appendix B: HASEL Production



Findings:

Laser settings work in a straight line
Laser pulsates at low voltages (because of PiD controls), therefore on smalles subjects the power is difficult to regulate. Therefore bumps and airbubbles also become more influential on the final result. Distance to focal point of the laser is very important, when a bubble or other irregularity in the surface is present, the laser gets unfocused.
Laser starts at lower power incorner and stops just before corner when dealing with small dimensions, so that it does not overshoot. Extending the lines in the dxf file can solve this, but corners remain fragile points in the structure. This can be worked around by rounding off corners, but again the laser finds it difficult to modulate this, since directing across the radius in y and x direction goes in small increments (steps).
At the discovered ideal settings, longer lines seem to work best in the middle. It might be an idea to make a raster of multiple squares and lines to try and get the ideal adhesion.

Appendix B: HASEL Production

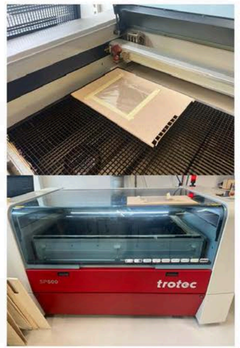

Two BOPP sheets on top of each other in the Laser cutter

After trying multiple setting, these were the ones that secured a good “weld”

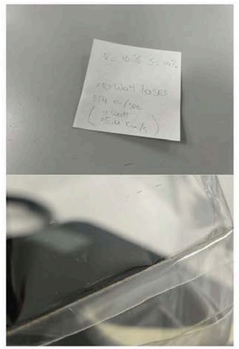

I went to the soldering station in the applied lab to test the method used by Mitchell et al. (2019) to solder two sheets together (to shut off a syringe cut out). This proved difficult to achieve because of the lack of Kapton sheet. At 160C it seemed somewhat achievable with short taps on the sheets, this temperature is the melting point of PP.

Appendix B: HASEL Production

After this initial test, I made another test setup. Again with two sheets, but this time a square cutout of 70 x 70 mm with a pocket of 50 x 50 inside and a 2mm cutout for a syringe. T

Using Iron & Flir

Tried to use iron at different heats to get a heatseal working. Unfortunately it seemed difficult to get a homogenous heat distribution across the aluminium with just the iron. Therefore, I went on to try the heat press at the Materials Lab.



Heat Press

In HASEL research reported by Kellaris et al. (2018), Heat press method is used.

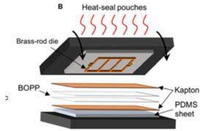

When trying with the heat press in the materials lab I found that this gives the best results. Therefore I had 3 shaped cnc’d out of aluminium in order to be able to quickly begin production.

Appendix B: HASEL Production





Appendix B: HASEL Production

References

Kellaris, N., Venkata, V. G., Smith, G. M., Mitchell, S. K., & Keplinger, C. (2018). Peano-HASEL actuators: Muscle-mimetic, electrohydraulic transducers that linearly contract on activation. *Science Robotics*, *3*(14). https://doi.org/10.1126/scirobotics.aar3276

Mitchell, S. K., Wang, X., Acome, E., Martin, T., Ly, K., Kellaris, N., Venkata, V. G., & Keplinger, C. (2019c). An Easy-to-Implement toolkit to create versatile and High-Performance HASEL actuators for untethered soft robots. *Advanced Science*, *6*(14). https://doi.org/10.1002/advs.201900178

P. Wissman, J. P., K. Ikei, A. K., Sampath, K., & A. Rohde, C. A. (2020). Hydraulically Amplified Self-Healing ELectrostatic (HASEL) Inspired Actuators. *Acoustics Signal Processing and Systems Branch.*

Appendix C: Requirements

Requirements	Description	Explanation/additional information
1. Technical Requirements		
1.1 Operation Range		
1.1.1	The system shall provide 60mm of travel across y-axis of seat.	See figure 10 for axis system.
1.1.2	The system shall provide more than one area of adjustability inside the bolster.	
1.1.3	The contact patch of the system shall be similar to or larger than the current air cell.	
1.1.4	The system shall not provide travel over any axes other than the y-axis.	
1.2 Load Bearing Capacity		
1.2.1	The system shall support a minimum of 250N of force spread across the contact area.	
1.2.2	The system shall be able to offer 90% of travel at 250N of spread force.	
1.2.3	The system	
1.3 Adjustment Speed		
1.3.1	Actuation time of a single actuator must be <8s.	Adustment time is measured between 10% and 90% travel
1.3.2	Actuation time of a single locking mechanism shall be <1s.	
1.4 Mechanism		
1.4.1	The system shall fit inside the bolster area of the seat including other material layering	
1.4.2	The system shall rely on shape memory alloy for its actuation.	
1.4.3	The system shall have a locking mechanism to mechanically lock its position.	
1.4.4	The locking mechanism shall rely on shape memory alloy for its actuation.	
1.5 Fixation		
1.5.1	The system and its individual modules are fixated to the bolster mounting of the seat frame.	
1.5.2	The system shall be fixated with the use of snap-on connections.	
1.6 Operation		
1.6.1	The system shall acieve this actuation time at an ambiet temperature of at least 20C.	
1.6.2	The system shall be able to operate with the use at a minimum of 12V.	
1.6.3	The system must work properly at no more than 3A current per actuation module.	
1.6.4	The system shall have an active eliment to detect pressure distribution on the contact area.	
1.6.5	The system shall autonomously respond to pressure distribution read outs.	
2. Materials		
2.1 Construction		
2.1.1	The system must consist of durable materials.	
2.1.2	The design of the system must be optimized to offer a lightweight construction.	
2.1.3	The materials used must be cost-effective for their application.	
2.1.4	The shape memory alloy used for actuation shall be NiTi wire.	
2.1.5	The system shall use TPU structures as a padding materials	
3. Comfort		
3.1 Adjustability		
3.1.1	The system shall offer enough adjustability to accomodate 95th percentile of population.	
3.1.2	The system shall offer adjustability in "just noticeable difference" increments.	Reference
3.2 Load Distribution		
3.2.1	The system shall distribute load through activation of the different SMA modules.	
3.2.2	The system shall have a TPU suspension layer tuned to peak load estimations.	
3.4 Operation		
3.4.1	The system shall be near noise-less in operation.	
3.4.2	The system shall works autonomously in adjustment.	
3.4.3	The user shall have the ability to set a preffered shape of the bolster.	
4. Safety		
4.1 General Safety		
4.1.1	The system shall have a fail-safe mechanism that brings the bolster to a default state in case of failure.	
4.1.2	The user shall have the ability to manually override the bolster shape.	
4.1.3	The temperature of the SMA actuator shall not exceed 120C.	Reference
4.1.4	The moving components shall be inclosed to offer edge protection.	
4.1.5	The systems shall have overload protection to protect the active elements.	
4.1.6	The system shall have temperature monitoring to prevent overheating.	
5. Sustainability		
5.1 Life Cycle		
5.1.1	The system shall have a life cycle of at least two years or 20.000 operation cycles.	
5.2 Repairability		
5.2.1	The system must offer the ability to quickly remove individual modules for replacement.	
5.2.2	Parts most prone to wear must be easily accessible for maintenance.	
5.3 Recyclebility		
5.3.1	The system shall not contain any PU or other composite foams to serve as a padding material.	
5.3.2	All parts shall be designed for easy disassembly at end of life.	
5.3.3	All materials used shall be recycleble or reusable at end of life.	
5.4 Efficiecy		
5.4.1	The system shall be designed to work as energy efficiently as possble.	
5.4.2	The design of all mechanisms should prioritize simplicity whenever possible.	
5.4.3	In operation, the time under power should be kept to a minimum.	
5.4.4	The system must have a minimal standby power consumption.	

Appendix D:
Informed Consent & Questionnaire

Participant number: _____

Bolster Pressure Distribution Test

This research is conducted as part of the MSc study Integrated Product Design at TU Delft.

Student: Max Nijhuis

Informed consent participant

I participate in this research voluntarily.

I acknowledge that I received sufficient information and explanation about the research and that all my questions have been answered satisfactorily. I was given sufficient time to consent my participation. I can ask questions for further clarification at any moment during the research.

I am aware that this research consists of the following activities:

1. Recording of general information and anthropometric data such as age, gender, height and weight.
2. Sitting in a near static position for 15 minutes uninterrupted.
3. Recording of pressure distribution of the participants body on the car seat.

I am aware that data will be collected during the research, such as notes, photos, video and/or audio recordings. I give permission for collecting this data and for making photos, audio and/or video recordings during the research. The data will only be accessible to the researcher, TU Delft supervisors and Jaguar Land Rover.

The photos, video and/or audio recordings will be used to support analysis of the collected data. The video recordings and photos can also be used to illustrate research findings in publications and presentations about the project.

I give permission for using photos and/or video recordings of my participation:
(select what applies for you)

- ☐ in which I am recognisable in publications and presentations about the project.
- ☐ in which I am not recognisable in publications and presentations about the project.
- ☐ for data analysis only and not for publications and presentations about the project.

I give permission to store the data for a maximum of 5 years after completion of this research and using it for educational and research purposes.

I acknowledge that no financial compensation will be provided for my participation in this research.

With my signature I acknowledge that I have read the provided information about the research and understand the nature of my participation. I understand that I am free to withdraw and stop participation in the research at any given time. I understand that I am not obliged to answer questions which I prefer not to answer and I can indicate this to the research team.

I will receive a copy of this consent form.

_____ _____

Last name First name

___ / ___ /___ _____

Date (dd/mm/yyyy) Signature

Participant Number: .....

Questionnaire

Objective:

The objective of this study is to analyze the pressure distribution on the bolster of a car seat when a participant sits in it for 15 minutes. The study aims to gather insights into comfort, support, and potential areas of improvement in the design of an shape morphing adjustable bolster system. The study specifically focuses on comfort provided by the seat, discomfort caused by the seat and performance of support (to the body) offered.

General Data

Age : .....

Gender: .....

Height: .....

Weight: .....

Please fill out the following questions.

How would you rate the overall comfort of the car seat on a scale of 1 to 7, with 1 being very uncomfortable and 7 being very comfortable?

Very Uncomfortable	*Uncomfortable*	*Slightly uncomfortable*	*Neutral*	*Slightly comfortable*	*Comfortable*	*Very comfortable*
1	*2*	*3*	*4*	*5*	*6*	*7*

Were there any specific areas on the bolster where you felt discomfort or pressure points? If yes, please describe.

.....

Did you find the support provided by the car seat adequate for your body? If not, please specify areas where improvement is needed.

.....

Participant Number: .....

Do you have any previous experiences with the comfort of side bolsters in car seats?

.....

Do you have any additional comments or suggestions regarding the car seat and your experience during the study?

.....

Appendix E: Arduino Code

```ino
const int pressureSensorPins[] = {A0, A1, A2, A3, A4, A5}; // Pressure sensor pins
const int actuatorPins[] = {2, 3, 4, 5, 6, 7}; // Actuator pins
const int numSensors = 6;
const int thresholdValue = 180; // Threshold value for triggering actuation

void setup() {
  Serial.begin(9600);
  for (int i = 0; i < numSensors; i++) {
    pinMode(pressureSensorPins[i], INPUT);
    pinMode(actuatorPins[i], OUTPUT);
  }
}

void loop() {
  for (int i = 0; i < numSensors; i++) {
    int sensorValue = analogRead(pressureSensorPins[i]);
    Serial.print("Sensor ");
    Serial.print(i + 1);
    Serial.print(" (A");
    Serial.print(i);
    Serial.print("): ");
    Serial.print(sensorValue);
    Serial.print("\t");

    if (sensorValue > thresholdValue) {
      if (i == 0) {
        digitalWrite(actuatorPins[1], HIGH); // Activate actuator 2
        digitalWrite(actuatorPins[2], HIGH); // Activate actuator 3
      } else if (i == numSensors - 1) {
        digitalWrite(actuatorPins[3], HIGH); // Activate actuator 4
        digitalWrite(actuatorPins[4], HIGH); // Activate actuator 5
      } else {
        digitalWrite(actuatorPins[i - 1], HIGH); // Activate previous actuator
        digitalWrite(actuatorPins[i + 1], HIGH); // Activate next actuator
      }
      delay(8000); // Actuation duration
      for (int j = 0; j < 5; j++) {
        digitalWrite(actuatorPins[j], LOW); // Deactivate all actuators
      }
    }
  }
  Serial.println();
}
```


Appendix F: Signed Project Brief

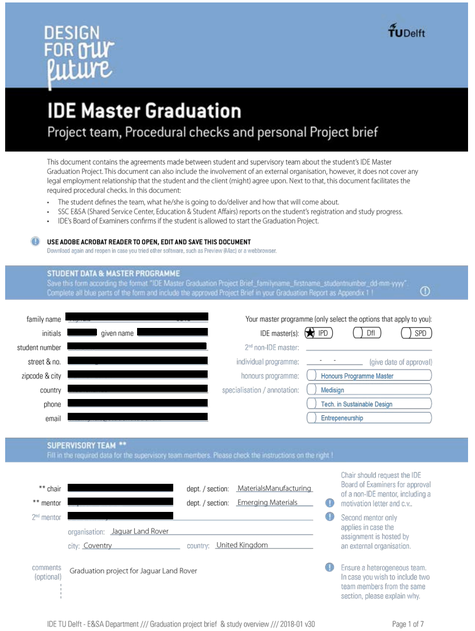

DESIGN FOR our future

TU Delft

IDE Master Graduation

Project team, Procedural checks and personal Project brief

This document contains the agreements made between student and supervisory team about the student's IDE Master Graduation Project. This document can also include the involvement of an external organisation, however, it does not cover any legal employment relationship that the student and the client (might) agree upon. Next to that, this document facilitates the required procedural checks. In this document:

- The student defines the team, what he/she is going to do/deliver and how that will come about.
- SSC E&SA (Shared Service Center, Education & Student Affairs) reports on the student's registration and study progress.
- IDE's Board of Examiners confirms if the student is allowed to start the Graduation Project.

USE ADOBE ACROBAT READER TO OPEN, EDIT AND SAVE THIS DOCUMENT
Download again and reopen in case you tried other software, such as Preview (Mac) or a webbrowser.

STUDENT DATA & MASTER PROGRAMME
Save this form according the format "IDE Master Graduation Project Brief_familyname_firstname_studentnumber_dd-mm-yyyy".
Complete all blue parts of the form and include the approved Project Brief in your Graduation Report as Appendix 1 !.

family name: [redacted]
initials: [redacted] given name: [redacted]
student number: [redacted]
street & no.: [redacted]
zipcode & city: [redacted]
country: [redacted]
phone: [redacted]
email: [redacted]

Your master programme (only select the options that apply to you):
IDE master(s): ★ IPD ○ DfI ○ SPD
2nd non-IDE master:
individual programme: - - (give date of approval)
honours programme: ○ Honours Programme Master
specialisation / annotation: ○ Medisign ○ Tech. in Sustainable Design ○ Entrepeneurship

SUPERVISORY TEAM **
Fill in the required data for the supervisory team members. Please check the instructions on the right !

** chair: [redacted] dept. / section: MaterialsManufacturing
** mentor: [redacted] dept. / section: Emerging Materials
2nd mentor: [redacted]
organisation: Jaguar Land Rover
city: Coventry country: United Kingdom
comments (optional): Graduation project for Jaguar Land Rover

Chair should request the IDE Board of Examiners for approval of a non-IDE mentor, including a motivation letter and c.v..
Second mentor only applies in case the assignment is hosted by an external organisation.
Ensure a heterogeneous team. In case you wish to include two team members from the same section, please explain why.

IDE TU Delft - E&SA Department /// Graduation project brief & study overview /// 2018-01 v30 Page 1 of 7

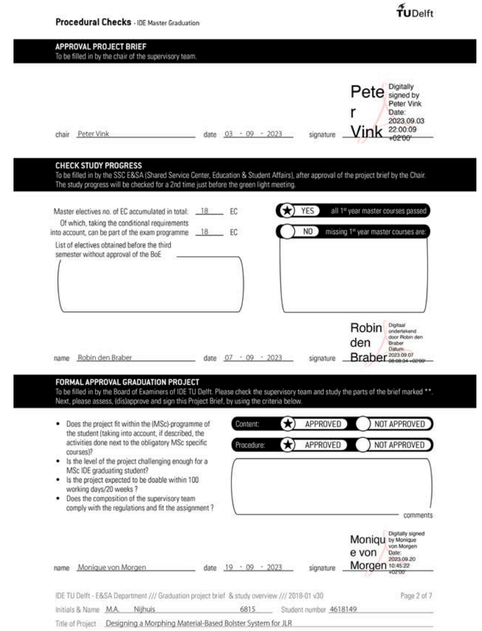

TU Delft

Procedural Checks - IDE Master Graduation

APPROVAL PROJECT BRIEF
To be filled in by the chair of the supervisory team.

chair Peter Vink date 03 - 09 - 2023 signature Peter Vink Digitally signed by Peter Vink Date: 2023.09.03 22:00:09 +02'00'

CHECK STUDY PROGRESS
To be filled in by the SSC E&SA (Shared Service Center, Education & Student Affairs), after approval of the project brief by the Chair.
The study progress will be checked for a 2nd time just before the green light meeting.

Master electives no. of EC accumulated in total: 18 EC
Of which, taking the conditional requirements into account, can be part of the exam programme: 18 EC
List of electives obtained before the third semester without approval of the BoE:

★ YES all 1st year master courses passed
○ NO missing 1st year master courses are:

name Robin den Braber date 07 - 09 - 2023 signature Robin den Braber Digitaal ondertekend door Robin den Braber Datum: 2023.09.07 09:08:34 +02'00'

FORMAL APPROVAL GRADUATION PROJECT
To be filled in by the Board of Examiners of IDE TU Delft. Please check the supervisory team and study the parts of the brief marked **.
Next, please assess, (dis)approve and sign this Project Brief, by using the criteria below.

- Does the project fit within the (MSc)-programme of the student (taking into account, if described, the activities done next to the obligatory MSc specific courses)?
- Is the level of the project challenging enough for a MSc IDE graduating student?
- Is the project expected to be doable within 100 working days/20 weeks ?
- Does the composition of the supervisory team comply with the regulations and fit the assignment ?

Content: ★ APPROVED ○ NOT APPROVED
Procedure: ★ APPROVED ○ NOT APPROVED
comments

name Monique von Morgen date 19 - 09 - 2023 signature Monique von Morgen Digitally signed by Monique von Morgen Date: 2023.09.20 10:45:22 +02'00'

IDE TU Delft - E&SA Department /// Graduation project brief & study overview /// 2018-01 v30 Page 2 of 7
Initials & Name M.A. Nijhuis 6815 Student number 4618149
Title of Project Designing a Morphing Material-Based Bolster System for JLR

Personal Project Brief - IDE Master Graduation

TU Delft

Designing a Morphing Material-Based Bolster System for JLR — project title

Please state the title of your graduation project (above) and the start date and end date (below). Keep the title compact and simple. Do not use abbreviations. The remainder of this document allows you to define and clarify your graduation project.

start date 04 - 09 - 2023 — 02 - 02 - 2024 end date

INTRODUCTION **

Please describe, the context of your project, and address the main stakeholders (interests) within this context in a concise yet complete manner. Who are involved, what do they value and how do they currently operate within the given context? What are the main opportunities and limitations you are currently aware of (cultural- and social norms, resources (time, money…), technology, …)

This document describes the direction for my graduation project for the Integrated Product Design master at Delft University of Technology.

During this graduation project it is my aim to combine different topics that I have worked on throughout my studies into one project in collaboration with Jaguar Land Rover.

In addition, this is a final chance deep-dive into interesting topics (while being at university) that I want to learn more about. Specifically, the topics I want to combine are: Ergonomics in design, human-centered design, (automotive) engineering, mechatronics & material science.
My interest in these areas both comes from my working experience and previous study projects where I learned about the integration of these subjects in a human mobility application.

An example of a relevant project I have worked on is the Alba Seat for the Advanced Embodiment Design course. During this course our team designed the first human-contour based lightweight airplane seat for short haul flights.

The Project

The assignment I would like to work on is based around pneumatic bolstering systems that support occupants of vehicles in lateral direction.

Currently, there are several OEMs already using this technology in their vehicles. However, it seems that these systems often rely on pneumatic hardware that is heavy, requires much electricity to work and generally have a high number of individual components that can go wrong.

My aim is to explore the performance of the current system and research application of morphing materials to counter any weaknesses, while also working to design a system that can offer comfort to a wide variety of users. The project will be based on human-centered design.
During Dave Withey's presentation at the IDE faculty before the summer I saw many similarities between the "morphable smart seat" and what I wish to do during my own project. For me, it is therefore very helpful to have support from JLR on this project, firstly because of the broad knowledge and resources they have and to see what it is like being part of a seating project in collaboration with a large automotive manufacturer.

Stakeholders

There are two main stakeholders in this project:

Main: Car occupants (Driver and front row passengers, perhaps all passengers in autonomous applications)

Secondary: JLR and manufacturers of "smart" alloys/polymers.

space available for images / figures on next page

Personal Project Brief - IDE Master Graduation

TU Delft

introduction (continued): space for images

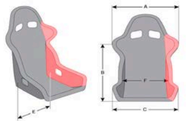

In red: Upper and lower side bolsters of a car seat. These are meant to keep the passenger snugly fitted in the seat during lateral acceleration.

Demonstration of active side bolster:
https://www.youtube.com/watch?v=HO3pyJhbLpA&t=305s



image / figure 1: Description of car seat bolsters

Race car (bucket) seats have extreme side bolsters to handle the high g-forces. In regular passenger cars the use of seats can vary from casual driving to a more dynamic style. Car manufacturers try to accomodate this by offering high adjustability in their seats. The way this is done currently this leads to complex systems with relatively high power usage.



High complexity in the 2019 mercedes s-class: 19 individual air chambers (per seat) that can adjust seat shape.



The 2023 Range Rover SV offers high levels of adjustability for both front-row and back-row seats.

image / figure 2: Bolsters and their adjustability.

Personal Project Brief - IDE Master Graduation

TU Delft

PROBLEM DEFINITION **

Limit and define the scope and solution space of your project to one that is manageable within one Master Graduation Project of 30 EC (= 20 full time weeks or 100 working days) and clearly indicate what issue(s) should be addressed in this project.

Current seat bolstering systems are complex (with many components "to go wrong") and energy-intensive devices. Since the introduction of these systems there has been much innovation in the field of (smart) materials, however, there seem to be no alternatives that perform better in these areas available than the conventional system yet. In addition, the current systems seem to be slow in their ability to adjust their shape and are limited by the shape and size of the airbags inside the seat that are shaping the bolsters.

My research will focus on using a combination of the most recent technical (smart morphing materials, mechanic structures) and non-technical solutions to improve the current system. Using less material and individual components while offering an improvement in function.

In order to improve on the current system there needs to be a clear reduction in complexity and increase in functionality. One of the main challenges will therefore be to consider different load cases of the system and determine in what way a smart morphing material, perhaps in addition with other structural components can handle the same loads as a pneumatic system.

As a final remark, to do this project within the 20 weeks given, it is important to set clear limitations on the scope of my research. A choice of material usage is therefore made early on in the project to help with direction in the prototype phase and come up with a feasible working prototype to present in the end.

ASSIGNMENT **

State in 2 or 3 sentences what you are going to research, design, create and / or generate, that will solve (part of) the issue(s) pointed out in "problem definition". Then illustrate this assignment by indicating what kind of solution you expect and / or aim to deliver, for instance: a product, a product-service combination, a strategy illustrated through product or product-service combination ideas, …. In case of a Specialisation and/or Annotation, make sure the assignment reflects this/these.

My project will be focused on recreating the current bolstering system using smart morphing materials to have it consume less energy. It will be based on relevant use cases, such autonomous, and dynamic driving. This also leaves room for exploring potential new applications/functions of the system.

To do this, the project will start out with setting a clear baseline that my system will improve upon. This baseline describes the performance of the current system with regards to its ability to handle different loads in its life cycle, its energy consumption, and its ability to accommodate for different body types.
While researching the use of morphing materials to recreate the adjusting bolsters the aim is therefore to reduce the use of electricity and improve ergonomics capabilities.

The expected result is to have a working physical prototype to showcase the feeling and working mechanisms of bolsters. In addition, I aim to collect convincing data to explain any advantages/disadvantages of my system in comparison to current systems.

The focus of this project will be on the mechanical (including material properties) layout of the system and user centered (ergonomic) design, while considering sustainability and brand identity of JLR.

Personal Project Brief - IDE Master Graduation

TU Delft

PLANNING AND APPROACH **

Include a Gant Chart (logistics like example below - more examples can be found in Manual 2) that shows the different phases of your project, deliverables you have in mind, meetings, and how you plan to spend your time. Please note that all activities should fit within the given net time of 30 EC = 20 full time weeks or 100 working days, and your planning should include a kick-off meeting, mid-term meeting, green light meeting and graduation ceremony. Illustrate your Gantt Chart by, for instance, explaining your approach, and please indicate periods of part-time activities and/or periods of not spending time on your graduation project, if any, for instance because of holidays or parallel activities.

start date 4 - 9 - 2023 — 2 - 2 - 2024 end date

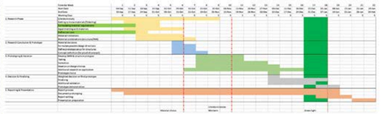

Personal Project Brief - IDE Master Graduation

TU Delft

MOTIVATION AND PERSONAL AMBITIONS

Explain why you set up this project, what competences you want to prove and learn. For example: acquired competences from your MSc programme, the elective semester, extra-curricular activities (etc.) and point out the competences you have yet developed. Optionally, describe which personal learning ambitions you explicitly want to address in this project, on top of the learning objectives of the Graduation Project, such as: in depth knowledge a on specific subject, broadening your competences or experimenting with a specific tool and/or methodology, ... Stick to no more than five ambitions.

Part of my drive to study Industrial Design Engineering has to do with my passion for cars and their (both technical and aesthetic) design. Initially, I always thought my goal would be to design the exterior of vehicles, but over time I have found that there are parts of these vehicles that fascinate me much more.
Being taught about human-centered design, I started looking at vehicles as products with humans at the center. This showed me that there is much going on between the car and driver, but there are only 3 main points of contact between them: the steering wheel, the pedals, and the seat.

Having done multiple projects on race car cockpit configurations and a project on airplane seat design, I became intrigued by how much impact just a seat can have on the overall experience of its user. To me, it feels like this is something that's often overlooked when I hear others talking about cars but might be one of the most important aspects of how people perceive it!

When Peter Vink brought me in contact with Dave Withey from JLR and we discussed the possibility of a graduation project, I proposed the project described above. To get a positive reaction and have their support to explore this relatively new topic for such a company in a field where currently much is changing (because of autonomous driving), is very exciting to me.

It seems almost a logical conclusion to my studies to finish with a project where I can combine my interests in design, cars and engineering. This also goes hand in hand with my wish to have a physical product to work on and using my hands in doing so, as this is also something I would always want to be doing wherever I work.

My ambitions for this project are as follows:
Firstly, to broaden my knowledge on (smart) materials. I wish to be the kind of designer that works on physical products, to be able to use and understand different materials I something I feel I must learn more about. This project allows me to experiment and learn on this subject.
Secondly, to get to know how it is to work with a large automotive OEM. As said, the topic of cars is a big motivator for me, but I feel I still must learn how it is to work with/for a car brand. During my graduation I hope to get a better feel for this.
Finally, to challenge myself in doing this project in a structured manner start to finish. In the past I struggled with planning and oversight on larger projects. Having the sole responsibility for the outcome of my graduation it seems as an opportunity to prove to myself that even though I can sometimes lose track or fall behind planning, I can reach my desired goals.

To conclude, I am excited to start on this project where I can prove what I already know as a designer, while also learning and showing my ability to overcome new challenges that are presented using theory and practice learned over the past years.

FINAL COMMENTS

In case your project brief needs final comments, please add any information you think is relevant.

Initials & Name M.A. Nijhuis 6815 Student number 4618149

Title of Project Designing a Morphing Material-Based Bolster System for JLR